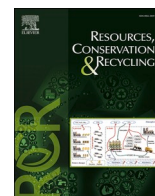




Contents lists available at ScienceDirect

Resources, Conservation & Recycling

journal homepage: www.sciencedirect.com/journal/resources-conservation-and-recycling

Full length article

Weakening of forest carbon stocks due to declining Ecosystem Photosynthetic Efficiency under the current and future climate change scenarios in India

Rahul Kashyap , Jayanarayanan Kuttippurath *

CORAL, Indian Institute of Technology Kharagpur, Kharagpur 721302, India



ARTICLE INFO

Keywords:

Carbon cycle
Ecosystem photosynthetic efficiency
Forest resilience
Machine learning
CMIP6
Dynamic global vegetation model (DGVM)

ABSTRACT

Despite lying in the tropics of higher carbon uptake, Indian forest carbon stocks are underexplored. We investigate the translation of greenness to carbon uptake (Ecosystem Photosynthetic Efficiency, EPE) and its impact on forest carbon (CUE) and water use (WUE) efficiencies in the current and future climate. We find hindered ability of Indian forests to translate greening into carbon uptake, due to a marked decline (-5 %) in EPE during recent decade (2010–2019) from the previous (2000–2009). The reduced EPE deteriorates forest health [(CUE, -4.5 %), (WUE, -3 %)] driven by soil drying (-2 %) and enhanced evaporative stress (+8 %). Granger Causality and Random Forest (RF) analyses reveal soil moisture (SM) as the key driver of EPE. Only 16 % of the Indian forests exhibits high integrity due to anthropogenic interventions. The CMIP6 and LPJ-GUESS model projections suggest weakening of forest carbon sinks in India and calls for sustainable actions to achieve the target of net-zero emissions by 2070.

1. Introduction

The stability of global climate system and carbon cycle is controlled by terrestrial ecosystems as they act as major carbon sinks, regulate the fluxes of carbon, water, energy and momentum between the land and atmosphere, and are home to vast varieties of habitats (Friedlingstein et al., 2024; Bar-On et al., 2025). Forests act as global carbon sinks, capturing almost 50 % of fossil-fuel emissions with tropical forest deforestation and degradation releasing almost 2/3rd of it (Pan et al., 2024). Thus, forests capture around 30 % of the anthropogenic carbon dioxide (CO₂) emissions (Ruehr et al., 2023; Bar-On et al., 2025). Therefore, utilising the carbon sequestration capacity of forests is a crucial element of strategies to alleviate climate change and a fundamental aspect of policy development (IPCC, 2021; Friedlingstein et al., 2024). Simultaneously, climate change in the warming world and enhanced dryness stress have adverse impacts on forests (Bauman et al., 2022; Yan et al., 2025). In the future, global warming will intensify aridity stress, which would decrease vegetation greenness, carbon uptake and perturb the terrestrial carbon cycle (Reichstein et al., 2013; Seneviratne et al., 2021).

Global carbon sinks have been stable for past three decades

(1990–2019) with regional biome level changes such as gain in temperate, and decline in boreal and tropical intact forests (Pan et al., 2024; Feng et al., 2024). However, growing climatic extremes (Tao et al., 2022; Feng et al., 2024), accelerated tropical deforestation (Qin et al., 2021; Zhao et al., 2024) and ageing forests (Yang et al., 2023) could disrupt the land carbon sinks (Pan et al., 2024). India lies in the tropical regions of higher carbon uptake and contributes about 7 % to the global carbon sinks (Harris and Gibbs, 2021), even with its mere 2 % of the global forest cover (ISFR, 2021). India reports 21.71 % of land area as forests and is the 8th largest in terms of global forest cover (ISFR, 2021). Additionally, India hosts 4 of the 36 biodiversity hotspots, and 2 of 8 hottest biodiversity hotspots in the world (Kong et al., 2021). Concurrently, India is the second largest contributor to the global greening (Chen et al., 2019) and one of the hotspots of land-atmosphere coupling (Humphrey et al., 2021).

India has been greening in recent decades due to climate change (Parida et al., 2020; Kashyap et al., 2022, 2023a) and anthropogenic activities (Kuttippurath and Kashyap, 2023). However, this is largely (86.5 %) cropland-based driven by improved irrigation and better land management (Kuttippurath and Kashyap, 2023). Some recent studies report mismatch in the greening and carbon uptake (Sarmah et al., 2021;

* Corresponding author.

E-mail address: jayan@coral.iitkgp.ac.in (J. Kuttippurath).<https://doi.org/10.1016/j.resconrec.2025.108478>

Received 8 July 2024; Received in revised form 15 June 2025; Accepted 19 June 2025

Available online 26 June 2025

0921-3449/© 2025 Elsevier B.V. All rights reserved, including those for text and data mining, AI training, and similar technologies.

Das et al., 2023) and carbon sink regions (Kashyap et al., 2023a) in India. Also, the carbon uptake by Indian ecosystems is projected to decline in the future climate scenarios (Bejagam et al., 2024). This calls for a dedicated study that thoroughly investigates the translation of greenness to carbon uptake in Indian forests and its drivers in the current and future climate scenarios. However, the translation of greenness to carbon uptake is rather complex (Walther et al., 2016; Zeng et al., 2023), as the photosynthesis and carbon uptake are very sensitive to environmental changes (Walther et al., 2016; Yan et al., 2019). Environmental factors have the potential to cause a substantial change in the carbon uptake even before inflicting any observable change in the vegetation greenness (Wei et al., 2022; Zhang et al., 2024). Ecosystem Photosynthetic Efficiency (EPE) is a metric used to understand this intricate relationship between greenness and carbon uptake (Zhang et al., 2024; Wang et al., 2023).

We, for the first time, estimate the translation of greenness to carbon uptake (EPE), and its impact on the health and functioning [Carbon Use Efficiency (CUE) and Water Use Efficiency (WUE)] of Indian forest ecosystems. We quantify the contribution, relation, association and sensitivity of ecosystem functioning metrics (EPE, CUE and WUE) to various climate drivers. Additionally, we estimate the resilience of forest carbon stocks to drying, warming, aridity and wildfires. We also unravel the anthropogenic influence on forest ecosystems in India. Apart from these, we examine the future of forest carbon stocks in India based on the Coupled Model Intercomparison Project Phase 6 (CMIP6) projection data and a process-based ecosystem model, Lund-Potsdam-Jena General Ecosystem Simulator (LPJ-GUESS), results. These findings will provide new insight into the complex relationship between greenness and carbon uptake. This will facilitate the implementation of strategic management and effective policies to preserve forest ecosystems, food security, achieve net zero target and to promote sustainability in India and other similar bioclimatic regions worldwide.

2. Data and methods

2.1. Data

2.1.1. Land cover, greenness, photosynthesis and carbon uptake

We utilise a wide range of datasets including satellite measurements and reanalyses as listed in Table S1. A synoptic scale observation for comprehensive monitoring of the terrestrial biosphere on a global scale are achieved through satellite remote sensing (Crowther et al., 2015; Chen et al., 2019). The effectiveness of moderate resolution imaging spectroradiometer (MODIS) for the tropical regions of high carbon uptake is well established (Sarmah et al., 2021; Kashyap et al., 2023a). Here, we utilise the MODIS Land Cover Type (MCD12Q1) Version 6 dataset that enables a comprehensive representation of global land cover types based on supervised classification of the surface reflectance data. Since this study is focused on forest ecosystems, we mask the other classes. The most widely used proxy of surface greenness is the Normalised Difference Vegetation Index (NDVI) as it represents vegetation vigour due to its association with chlorophyll content, foliar nitrogen and leaf characteristics of the plant (Parida et al., 2020; Kuttippurath and Kashyap, 2023). We utilise the MODIS MOD13A1 NDVI for this purpose. We also consider the biophysical metric, Leaf Area Index (LAI) based on MODIS MCD15A2H LAI as it is one of the key parameters to quantify the greenness and biomass of the ecosystem due to its close association with the plant biophysical processes (Chen et al., 2019; Kuttippurath and Kashyap, 2023). To effectively quantify the plant photosynthetic activity, it is crucial to estimate the fraction of photosynthetically active radiation (FPAR) that plants absorb from the solar energy (Kashyap et al., 2022, 2025). The NDVI-FPAR relation is linear in most cases and FPAR could be evaluated more accurately using NDVI as detailed in Supplementary material. We also utilise the Net Primary Productivity (NPP) from MODIS (MOD 17 A3HGF) as it is one of the most fundamental ecological variables used to quantify the plant carbon

uptake, measured as the residual of Gross Primary Productivity (GPP, MOD 17 A2HGF) after autotrophic respiration (Ra) (Nemani et al., 2003; Kashyap et al., 2023a). Additionally, we analyse the Solar-Induced Fluorescence (SIF) data from GOSIF v2 gridded dataset (Li and Xiao, 2019; Kashyap et al., 2023b). SIF is the radiation flux emitted as light energy in the wavelength range 650–800 nm during photosynthesis (Rascher et al., 2015) and is considered an efficient indicator of photosynthetic activity (Shekhar et al., 2022).

2.1.2. Ecosystem characteristics

The ecosystem characteristics taken in account are canopy cover, Vegetation Continuous Fields (VCF) and above ground biomass (AGB). The canopy cover is the proportion of the land that is having forest canopy represented in terms of percentage (%) for the year 2010 obtained from the Global Forest Watch (GFW). The Vegetation Continuous Fields (VCF) product is a comprehensive description of the Earth's surface, encompassing three distinct components of ground cover (tree, non-tree and bare) surfaces. Here, we consider MODIS VCF (MOD44B Version 6.1) as it is the primary dataset known as the percent tree cover layer that provide the percentage of each pixel covered by a tree canopy. The biomass is a measure of the carbon stock in the plant. Here we use the AGB data derived from GlobBiomass for the year 2010 (Santoro et al., 2021). We also consider the forest age data to examine the structure, carbon sequestration ability, recovery post-disturbance by climate change and anthropogenic intrusions of Indian forest ecosystems. These data are an ensemble of the global forest inventories, biomass and climate data and are obtained from the Max Planck Institute of Biogeochemistry (MPI-BGC) for the year 2010 (Besnard et al., 2021).

2.1.3. Meteorology, aridity, fire and topography

The moisture availability is assessed based on the precipitation (P) data from the Global Precipitation Measurement (GPM) and the soil moisture (SM) data from the Global Land Data Assimilation System (GLDAS). The aridity is quantified in terms of Climatic Water Deficit (CWD) and Vapour Pressure Deficit (VPD) obtained from the TerraClimate database. CWD is a measure of land evaporative aridity quantified as the difference between the potential evapotranspiration (PET) and actual evapotranspiration (AET). Basically, CWD is the amount of water that would have potentially evaporated/transpired to the atmosphere, if it was available (Huang et al., 2021; Kashyap and Kuttippurath, 2024a). VPD is a measure of atmospheric evaporative demand or atmospheric aridity as it is the difference between the saturated and ambient vapour pressure conditions at a particular temperature (Bauman et al., 2022). VPD is considered to have a strong control on the vegetation stomatal opening and thus influence the exchange of carbon and water between the biosphere and atmosphere (Bauman et al., 2022; Yan et al., 2025). The temperature (T) data is obtained from fifth generation European Centre for Medium-Range Weather Forecast Reanalysis (ERA-5). The evapotranspiration (ET) data are obtained from MODIS (MOD16 A3HGF) to account for ET and estimate WUE (Kashyap and Kuttippurath, 2024a, b). We also consider the fire counts from MODIS Fire Information for Resource Management System (FIRMS) to account for the impact of wildfires on the ecosystem health (Giglio et al., 2016; Kashyap and Pandey, 2021). To have a clear understanding of the impact of topography and terrain on the variability of forest types and their health, we utilise the elevation data based on the Advanced Space-borne Thermal Emission and Reflection Radiometer (ASTER) Global Digital Elevation 4 Model (GDEM) Version 3 (ASTGTM) data (Farr et al., 2007).

2.1.4. Anthropogenic activity

To account for anthropogenic influence on the forests we consider two indices, the Human Modification Index (HMI) and Forest Landscape Integrity Index (FLII) for the year 2016. HMI is obtained from the Socioeconomic Data and Applications Center (SEDAC) and it ranges from 0 to 1, which represents the cumulative measure of human modification

on land accounting for a total of 13 anthropogenic stressors divided into 5 categories such as (i) human settlement, (ii) agriculture, (iii) transportation, (iv) mining and energy production and (v) electrical infrastructure (Kennedy et al., 2019). FLII is the first estimate of ecological integrity of global forests, where it accounts for the observed and inferred human pressure (infrastructure, agriculture and tree cover loss) accounting for the loss of forest connectivity (ratio of current to potential forest connectivity), for the year 2019. It ranges from 0 to 10, where low is 0–6, moderate is 6–9.6 and high is 9.6–10 (Grantham et al., 2020). Furthermore, we also estimate the change in human population in the year 2019 from 2000, based on the pixel-wise image differencing technique, for the Indian forest regions, which is a proxy for examining the anthropogenic interventions in these natural ecosystems.

2.1.5. Future projections from the CMIP 6 models

We consider the future projection data for LAI, GPP, NPP and ET from the models CNRM (1.40° × 1.40°), ACCESS (1.875° × 1.25°), MPI-ESM (1.88° × 1.86°) and Can-ESM (2.81° × 2.77°), as these are high resolution models with good reliability for the Indian region (Bejagam et al., 2024). We use the data from high-resolution CMIP6 models such as GFDL, CNRM, CM61HR and HadGEM for P and T for high emissions scenarios (Shared Socioeconomic Pathways, SSP585) detailed in Table S2.

2.2. Methods

We use a suite of statistical techniques such as correlation, multiple linear regression (MLR), machine learning (ML) based Random Forest (RF) model, Granger Causality, Growth Rate (GR) estimation and Resilience method to make our analysis robust to draw solid conclusions. The key methodological approaches are given below.

2.2.1. Regional and spatio-temporal variability estimation

First, we present the spatial variability in the forest cover in India in terms of their broad geographic/climatic zones, forest types and elevation zones. Then, we present VCF, canopy cover and biomass and estimate their regional variability. Then, we compute the spatio-temporal variability in greenness, photosynthesis and productivity (FPAR, SIF, LAI and NPP). We utilise the image differencing technique to estimate the change in greenness, photosynthesis and productivity in recent decade (2010–2019) from its previous decade (2000–2009). The decadal change in moisture availability (P and SM), aridity (CWD and VPD) and T are also estimated using the Eq. (2):

$$\% X_{R-P} = \frac{X_R - X_P}{X_P} \times 100 \quad (1)$$

Here, X is any variable like LAI or NPP, R is the mean of X in recent decade (2010–2019), and P is the mean of X in the previous decade (2000–2009).

To delineate the regional variability in different bioclimatic regions, we estimate the normalised regional anomaly (NRA) of the changes in various variables, as per Eq. (2):

$$NRA = (I_m - X_m)/X_m \quad (2)$$

Here, I_m = mean change value for any bioclimatic forest region of India and X_m = mean change value for the Indian forests.

We estimate forest loss based on pixel-wise image differencing technique and the pixels of forest regions converted to non-forest pixels are delineated as “forest loss” based on MODIS Land Cover Type between the years 2001 and 2019.

2.2.2. Estimation of forest health and functioning

We estimate three metrics of ecosystem health and functioning namely, EPE, CUE and WUE. EPE is the translational ability of greenness to productivity by plants. It is computed as the ratio of SIF to LAI previously (Wei et al., 2022; Wang et al., 2023; Zhang et al., 2024).

However, being a weak signal, at times SIF is not accurately captured and is not always a surrogate for the amount of carbon assimilated by ecosystems particularly in high biomass regions like forests (MacBean et al., 2018; Zeng et al., 2023). Therefore, we estimate EPE as the ratio of carbon uptake (NPP) to greenness (LAI) for the forest ecosystems as per Eq. (3):

$$EPE = \frac{NPP}{LAI} \quad (3)$$

The ecosystem CUE is the measure of the rate or the ability of the vegetation to sequester carbon from the atmosphere (Gang et al., 2022; Kashyap et al., 2023a). It is basically the rate of conversion of GPP to NPP in ecosystems estimated as per Eq. (4):

$$CUE = \frac{NPP}{GPP} \quad (4)$$

The ecosystem WUE is the amount of carbon assimilated to the water lost through transpiration during photosynthesis by the plant (Keenan et al., 2013; Kashyap and Kuttippurath, 2024a). It is a key ecohydrological metric that interlinks the carbon and water cycles, and is estimated as per Eq. (5):

$$WUE = \frac{NPP}{ET} \quad (5)$$

We also compute the future EPE, CUE and WUE based on the future LAI, GPP, NPP and ET data from the model projections. We estimate the change EPE, CUE and WUE among the decades from the historical (2015–2019) to the future periods such as the decades of mid-century (2040–2050) and end-century (2090–2100).

2.2.3. Relation with drivers: Correlation and Granger Causality

To decipher the associations of drivers with EPE we perform Pearson's correlation analysis. However, since correlation does not imply causation, we further investigate the existence of causal relationships among EPE and its drivers based on Granger causality. We consider Granger causality test based on the concepts of "cause" and "effect". Granger causality is affirmed wherein the potential to predict future responses of variable Y enhances by accounting all relevant information, except for the present value of variable X (Granger, 1969) as detailed in Supplementary material. To conduct a Granger causality test, a bivariate model is established between the time series (X and Y) that are stationary as per Eqs. (6) and (7):

$$Y_t = \sum_{i=1}^n a_i Y_{t-i} + \sum_{i=1}^n b_i X_{t-i} + \varepsilon_t \quad (6)$$

$$X_t = \sum_{i=1}^n c_i X_{t-i} + \sum_{i=1}^n d_i Y_{t-i} + \delta_t \quad (7)$$

where, X and Y are two stationary time series; a, b, c and d are coefficients; and ε and δ are white noise. For X to Granger cause Y, $b_i \neq 0$; for Feedback between X and Y, $d_i \neq 0$. To comprehend the temporal delay in Granger Causality, a maximum lag of 4 months is assigned.

2.2.4. Contribution of drivers: Random Forest and MLR

The capability of machine learning (ML) to effectively handle multidimensional data has made it very useful for modelling systems that exhibit complex nonlinear structures. The Random Forest (RF) is an ensemble model that integrates boosting and regression trees (Breiman, 2001). A total of 500 trees are generated, with two variable splitting in each tree. These data are partitioned into two subsets: 30 % for testing and 70 % for training purposes. In this study, a methodology based on precision is employed to estimate the relative contribution of each driver on EPE, CUE, and WUE. In R Studio version 4.2.1, we employ the RF model along with the "randomForest" and "caret" packages to assess the relative significance of each variable based on independent data

samples. In RF, each tree has its own independent out-of-the-bag data sample that were not included in the initial build. The first step involves evaluating the specimen obtained directly from the bag in terms of its predictive accuracy. Afterwards, the stability of all other variables is maintained, while the values of the variables in the outlier sample are generated randomly. We assess the accuracy of predicted values by calculating the average decrease in precision across all trees. The value indicator is further divided into various categories of the outcomes. It can be deduced that the stochastic rearrangement of a variable leads to the total elimination of its predictive capability. The importance of a variable is a measure of the degree to which its omission results in a decrease of precision, as per Eq. (8):

$$I_x = \sum_{k=1}^K \left[\frac{1}{K} (MSE_k^{xprem} - MSE_k) \right] \quad (8)$$

Here, I_x is the variable importance or contribution, K is the number of trees in the forest, MSE_k^{xprem} is the estimation error with predictor x being eliminated for the k^{th} decision tree, and MSE_k is the forecasting error with all predictors included in the k^{th} decision tree.

The RF model's default hyperparameters are chosen for their exceptional efficiency in executing the algorithm (e.g. Kashyap and Kuttippurath, 2024a, b). Additionally, we employ MLR to estimate the influence of the drivers and complement the findings drawn from the RF model as explained in Supplementary material.

2.2.5. Sensitivity to drivers

We estimate the sensitivity of forest health and functioning (EPE, CUE and WUE) to its drivers such as P, SM, CWD, VPD, FPAR, T and fire count (FC) as per Eq. (9):

$$S_x = \frac{\Delta S}{\Delta X} \quad (9)$$

Here, S_x is the sensitivity of S to X , and S is either of EPE, CUE or WUE and X is its driver (P, SM, CWD, VPD, FPAR, T and FC). The change in S (ΔS) and X (ΔX) are the percentage change in recent decade (2010–2019) from the previous decade (2000–2009) (Kashyap et al., 2025).

2.2.6. Growth Rate analysis

The Growth Rate (GR) concept is widely used in economics to compute the intermediate variations and overall cumulative changes over a period. Recently, this technique has also been employed to investigate the atmospheric CO_2 concentration changes (Keenan et al., 2016). It is estimated as the difference in the value (X) in the current (t) from the previous ($t-1$) period, as shown in Eq. (10):

$$X_{GR} = X_t - X_{t-1} \quad (10)$$

Here, X_{GR} is the growth rate (GR) in X (EPE and its drivers) between time periods t and $t-1$.

We also estimate the cumulative growth rate (CGR, Eq. (11)) and mean growth rate (MGR, Eq. (12)) for the study period (2000–2019).

$$CGR = \sum_{i=1}^n X_{GR} \quad (11)$$

$$MGR = \left(\sum_{i=1}^n X_{GR} \right) / n \quad (12)$$

Here, n is the number of years of the study.

2.2.7. Forest Resilience

The ability or potential of an ecosystem to maintain its state and functioning amidst a disturbance is termed as resilience (Holling, 1973). Resilience method has gained a wide popularity in studies pertaining to ecosystems (Sharma and Goyal, 2018; Kashyap and Kuttippurath, 2024a). Here we, estimate the forest resilience to P drying, SM stress,

surface warming, CWD, VPD and wildfires. Since, it is a long-term analysis and we cannot consider every event as it would be for a small period and on a regional scale, we rely on the worst affected year. First, we find the largest negative anomaly (P and SM) and positive anomaly (CWD, VPD, T and fire count (FC)). Then, we compute the ratio (Ri) of the worst affected year (Y_x) to the overall mean of the period (Y_m). The non-dimensional quantity Ri is called as the coefficient of resilience as per Eq. (13):

$$R_i = \frac{Y_x}{Y_m} \quad (13)$$

The Ri threshold of 0.8–0.9 is moderately resilient, while higher than that is resilient and lower is non-resilient (Sharma and Goyal, 2018; Kashyap and Kuttippurath, 2024a).

2.2.8. Process based ecosystem model

LPJ-GUESS is a process based dynamic global vegetation model (DGVM) that analyses the dynamics of vegetation, biogeochemistry of the ecosystem and water cycling. By utilising available data on regional climate conditions and atmospheric CO_2 , it is possible to make predictions regarding the structural, compositional and functional properties of the indigenous ecosystems found within the primary climate zones of our planet. In LPJ-GUESS models trees as age cohorts that are identical within each cohort (age class) but differ across multiple replicate patches. It gives outputs such as the composition and coverage of vegetation, categorised by major plant functional types (PFTs) (Smith et al., 2014). We employ the LPJ-GUESS (version 3.0) model to estimate LAI, NPP, biomass, leaf carbon and nitrogen ratios (leaf C:N) for six selected forest sites in India, one each in six different bio-climatic regions, as detailed in Supplementary material (Table S3). We initially run the model for 1000 years as a “spin up” to tune the model up for each forest site and then run in the “transient phase” for 20, 50, and 100 years to match the periods of 2015–2019, 2040–2050, and 2050–2100, respectively. We use a pre-defined climate [(precipitation (P) and temperature (T)] through “Run GetClim” module, which uses default atmospheric CO_2 concentrations for the “spin up”. In the “transient phase”, we run the model initially for the “climate change” scenario. We employ the available P (GPM) and T (ERA-5 2 m) data to compute their anomaly for the period 2015–2019 and multi-model (GFDL, CNRM, CM61HR, HadGEM) ensemble of P and T from CMIP6 climate projections for the future runs i.e. 2040–2050, and 2050–2100. We also run the LPJ-GUESS model for “no-climate change” scenario when the P and T anomalies are set at 0.

3. Study area

3.1. Zones, PFTs and elevation

The forested ecosystems in India are spatially categorised into six bioclimatic regions: (i) Western Himalaya (WH), (ii) Eastern Himalaya (EH), (iii) North East (NE), (iv) Indo-Gangetic Plain (IGP), (v) Central India (CI), and (vi) Western Ghats and Peninsula (WGP) (Fig. S1a). Evergreen Needleleaf Forests (ENF) are found in the foothills of WH in the moderate elevation zones (600–1200 m). Evergreen Broadleaf Forests (EBF) are found mostly in EH, NE and western ghats (WG) in a wide range of elevations (600–2400 m). Deciduous Needleleaf Forests (DNF), are found in moderate elevation zones (600–1200 m) of lower WH and CI. Deciduous Broadleaf Forests (DBF) are majorly found in the low elevation areas (< 600 m) of CI, IGP and WGP. Mixed Forests (MF) are a blend of evergreen and deciduous tree types (40–60 % of each) found in all forested regions and are the predominant forest types in WH and EH in the high (1200–4800 m) elevation and CI in low (300–600 m) elevation areas (Fig. S1b, S1c)

3.2. Canopy, Vegetation Continuous Fields and biomass

For the Indian forests, we find the mean the canopy cover as 55.6 %, VCF as 52.5 % and AGB as 589 Mg/ha. In terms of spatial variability,

there is a homogeneous pattern among canopy, VCF and AGB (Fig. S1d, e, f). Among the regions, EH with forest types such as EBF and MF have the highest VCF (68.5 %), canopy (77.8 %) and AGB (786 Mg/ha). NE is the other region with EBF, MF and DBF, has high VCF (59 %), canopy

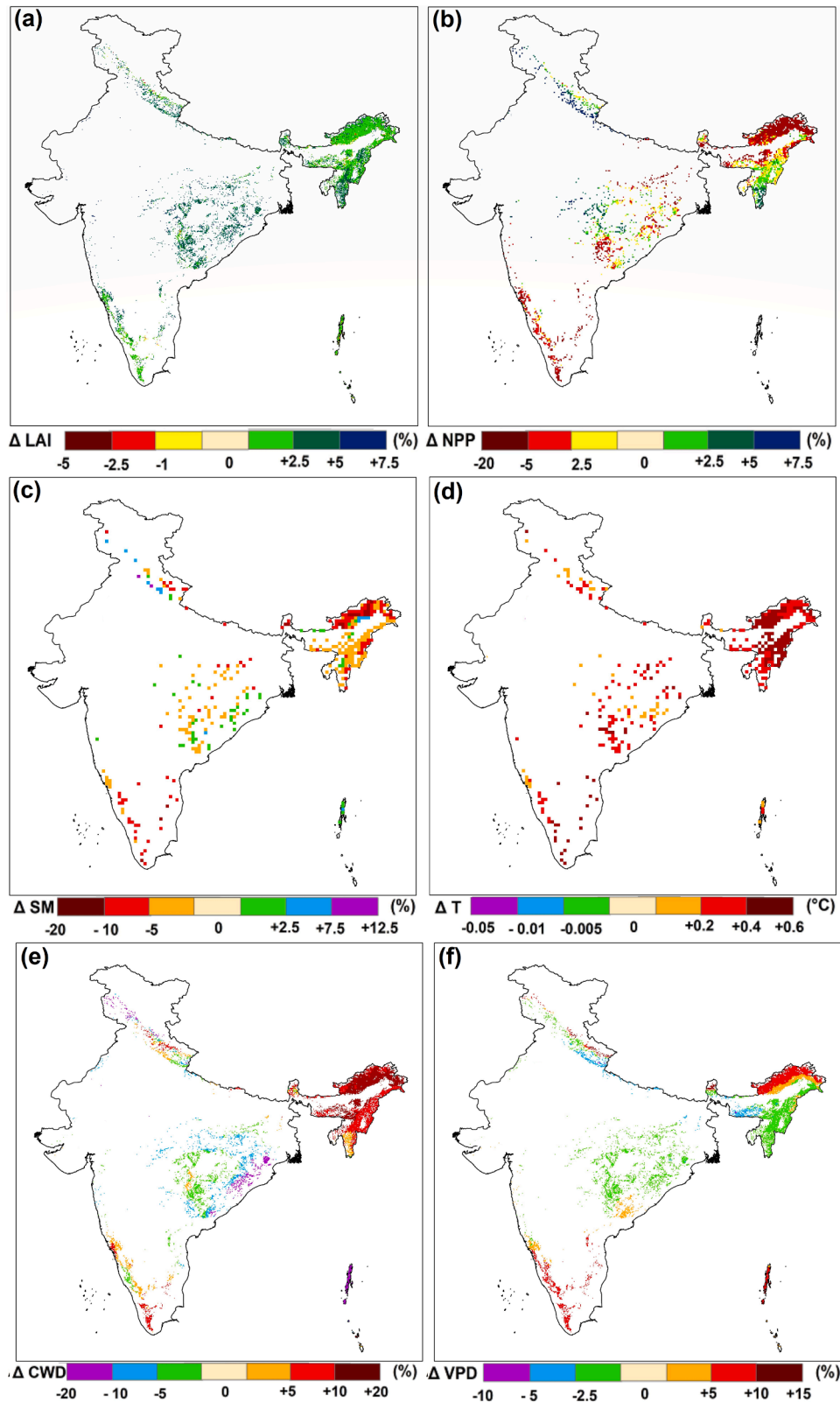


Fig. 1. Change (%) in (a) Leaf Area Index (LAI), (b) Net Primary Productivity (NPP), (c) Soil Moisture (SM), (d) Temperature (T), (e) Climatic Water Deficit (CWD) and (f) Vapour Pressure Deficit (VPD) in recent decade (2010–2019) from the previous decade (2000–2009) for Indian forests.

(69.8 %) and AGB (662 Mg/ha). WGP forests have high VCF (45 %) and canopy (50.7 %). In contrast, CI with forest types such as DBF and MF has the lowest VCF (29.7 %), canopy (36.4 %) and AGB (378 Mg/ha).

3.3. Greenness, photosynthesis, carbon uptake and climate

Here, high FPAR (0.75–0.9), SIF (0.3–0.4 W/m²/m/sr), LAI (5.5–7 m²/m²) and NPP (900–1500 gC/m²/yr) are observed in majority of the forested areas in EH, NE, and WGP (Fig. S2). These are the regions of high moisture availability [P (> 10 mm/day), SM (> 80 kg/m²)], moderate ET (750–1500 mm) and optimum T (16–25 °C). Moreover, these are also the regions of lower aridity [lower CWD (< 30 mm) and VPD (< 0.8 kPa)]. Contrarily, low FPAR (< 0.65), SIF (< 0.2 W/m²/m/sr), LAI (< 4.5) and NPP (< 500 gC/m²/yr) are exhibited by the forests in the south WH and majority of CI. Limited moisture availability [P (< 6 mm/day), SM (< 60 kg/m²)], lower ET (< 750 mm), higher T (> 25 °C) added by higher aridity [(CWD > 45 mm), (VPD > 1.3 kPa)] are the reasons for this (Figs. S3, S4). It is evident that the forest ecosystems with ample moisture availability, optimum warmth and lower aridity show higher greenness, photosynthetic activity and carbon uptake.

4. Results

4.1. Decline in forest carbon uptake despite greening

The forests in India experience a rise in FPAR (2.3 %), SIF (2.2 %) (Fig. S5), and LAI (3.1 %) (Fig. 1a) in recent decade (2010–2019) from the previous decade (2000–2009). In terms of spatial heterogeneity, large increase (2.5–7.5 %) in FPAR, SIF and LAI is observed in majority of forests in CI and some areas of WH. Marginal (< 2.5 %) increase in FPAR, SIF and LAI is found in some forests of WH, EH, NE and WGP. LAI exhibits an increase in all six bioclimatic regions, with its highest in WH (4 %) and WGP (2.9 %). Similarly, FPAR and SIF also show an increase in most regions; suggesting the greening of Indian forests. However, the forests in India experience a decline (–1.4 %) in carbon uptake (NPP) during recent decade from the previous (Fig. 1b). Substantial increase (2.5–7.5 %) in NPP is observed in some forest regions of WH, CI and NE, but marginal (< 2.5 %) increase in some areas of WH, NE and CI. This increase is overridden by large decline (–5 to –20 %) in NPP observed for most forests of EH, WGP and some in CI and IGP. Small (< –5 %) decline in NPP is found in some areas of NE, CI and WGP. In terms of regional heterogeneity, except for WH (0.3 %), all other regions exhibit decrease in NPP, and is prominent in EH (–1.8 %), WGP (–1.5 %) and IGP (–1.4 %). This decline in carbon uptake with hotspots in the pristine forests of EH and WGP is also in the regions of high SM stress (–20 to –5 %), intense warming (0.2–0.6 °C), and enhanced land (CWD) and atmospheric aridity (VPD), about 10–20 % (Fig. 1c, d, e, f)

In terms of the temporal variability (Fig. S6) there is a homogeneity among photosynthesis (FPAR), greenness (LAI), and carbon uptake (NPP) in the previous decade (2000–2009), but not in recent decade (2010–2019). While, FPAR, and LAI exhibit substantial recovery post-2012, NPP fails to do so. To find the reason for this, we investigate the temporal variability in NPP with its drivers (Figs. S6, S7) such as moisture availability (P and SM), temperature (T), ET, aridity (CWD and VPD). The year 2012 exhibits a marked decline in moisture availability, higher warming and large VPD that drives sharp reduction in NPP. The forest NPP recovered up to a certain extent in 2013, but then again declined in 2014 and continued to 2016 due to very high VPD in 2014. Since 2015, enhanced warming and ET deplete SM and thus, drive the reduction in forest carbon uptake. It suggests that enhanced greenness has not translated into carbon stocks by the forests in India, and this mismatch is stronger in the pristine forests of EH and WGP.

4.2. Forest health and drivers

To explore the reason for the inability of forests to translate greening

into carbon uptake, we examined the forest health and functioning metrics in terms of their photosynthetic ability (EPE, Fig. 2a), carbon sequestration (CUE, Fig. S8) and water use (WUE, Fig. S8). We find that the forests dominated by EBF in EH, NE and WGP have high (1250–2000) EPE. Conversely, low (< 750) EPE is found in the forests dominated by MF in the lower WH and CI. Most areas in CI and some areas in eastern peninsula dominated by DBF exhibit moderate (750–1250) EPE. Likewise, high (0.7–0.9) CUE is observed for forests in most regions of EH, some areas in WH, EH, NE and WGP dominated by MF and EBF. However, low (< 0.45) CUE is found in forests of lower WH and CI dominated by DBF. Very high (2–3) WUE is observed in forests of WH and EH dominated by MF. Forests in NE and WGP also exhibit large (1.5–2) WUE dominated by EBF, but majority of forests in CI and lower WH show low (< 0.75) WUE and are dominated by DBF.

We then investigate the relation of EPE with its drivers (Fig. S9) and find that SM (0.64) and T (–0.55) have strong positive and negative relations, respectively. CWD (0.41) and P (0.31) have the positive control, contrary to negative influence of VPD (–0.2) and ET (–0.14). We further explore the causal relationship of EPE with its drivers based on Granger Causality test at 0–4 months temporal lag (Fig. 2b). The results reveal that EPE has causal association with SM, T, ET, CWD and VPD. Interestingly, P has no direct causal relation with EPE, but influences EPE through other drivers such as SM and T. SM and T emerge as major drivers as they have causal link with other drivers. Furthermore, to quantify the control of various drivers, we estimate the relative importance based on RF (Fig. 2c). We find, the most dominant driver of EPE is SM (26.6 %), followed by VCF (19.4 %) and T (13.1 %). Amongst others, P (8.7 %), FPAR (8.7 %), VPD (8.6 %), VCF (8.4 %) and CWD (6 %) are very important to EPE variability. We also employ MLR to estimate the influence of drivers to EPE variability and find similar results to that of RF (Table S4). Likewise, SM is the key to the variability in both CUE (31.3 %) and WUE (32 %). Temperature also has a notable control on forest CUE (17.8 %) and WUE (16.8 %). FPAR and VCF are more important to the variability in CUE (14 %, 9.2 %) than WUE (10.7 %, 7.5 %). In contrast, VPD and P have a stronger control on WUE (12.6 %, 7.8 %) than CUE (11.2 %, 4.6 %), whereas CWD has a stronger control on CUE (5.3 %) than WUE (5.1 %) (Fig. S8).

4.3. Declining forest health

To understand the changes in health of forest ecosystems, we estimate the change (Fig. 3a, b, c), in EPE, CUE and WUE in recent decade (2010–2019) from the previous decade (2000–2009). The forests in India experience a notable decline in all three metrics of ecosystem health with the largest reduction in EPE (–5 %), followed by CUE (–4.5 %) and WUE (–3 %). In terms of spatial heterogeneity, a substantial decline (–5 to –20 %) in EPE is observed in most of EH, CI, WGP, IGP and some areas in NE. A small (< –5 %) decline in EPE is found in some areas of WH, NE and CI. Some areas in WH exhibit a large increase (2.5–7.5 %) in EPE and some areas in NE and CI show marginal (< 2.5 %) increase in EPE. Likewise, a substantial decline (–5 to –20 %) in CUE is observed in some areas of WH, EH, NE, CI and WGP. A small (< –5 %) decline in CUE is also found in some areas of WH, NE and CI. Some areas in WH exhibit a high increase (2.5–7.5 %) in CUE and some areas in CI find a marginal (< 2.5 %) increase in CUE. A substantial reduction (–5 to –20 %) in WUE is observed in most of WH, CI and some areas in NE. A small (< –5 %) decline in WUE is also found in some areas of EH, NE, CI and WGP. Some areas in EH, NE, IGP and eastern peninsula show an increase in WUE. In terms of temporal variability (Fig. 3d), there is an evident decline in all three (EPE, CUE and WUE) forest health metrics in recent decade (2010–2019). As found in NPP (Fig. S6), it never recovered after the big drop in 2012, with recurring reductions in 2014–2016 and 2019.

The decline in the health of Indian forests is due to reduced moisture availability [P (–1.1 %), SM (–2.2 %)], increased aridity [CWD (8.2 %) and VPD (0.4 %)], surface warming (0.125 % or 0.36 °C) and frequent

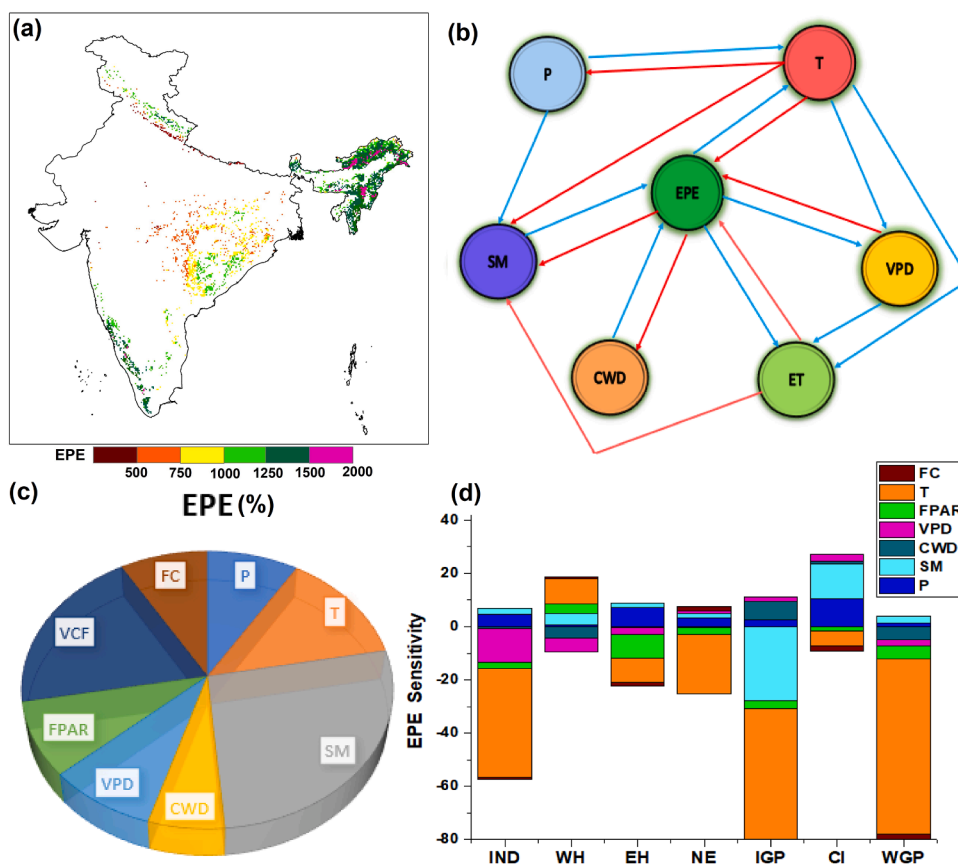


Fig. 2. (a) Ecosystem Photosynthetic Efficiency (EPE), (b) Granger Causality results for relation of EPE (blue line: positive impact, red line: negative impact) with drivers at 0–4 months temporal lag. (c) Random Forest based relative contribution (%) of drivers to EPE variability, (d) Sensitivity of EPE to its drivers- Precipitation (P), Soil Moisture (SM), Temperature (T), Climatic Water Deficit (CWD), Vapour Pressure Deficit (VPD), Fraction of Photosynthetically Active Radiation (FPAR), Vegetation Continuous Fields (VCF) and Fire Counts (FC) for Indian forests during the period 2000–2019.

wildfires (8.7 %) in recent decade (2010–2019) from the previous decade (2000–2009) (Fig. 3e). In terms of regional heterogeneity, all regions except WH [EPE (+7.2 %) and CUE (+12.3 %)], have reduced EPE and CUE. The regions such as EH (−9 %), WGP (−8 %) and IGP (−7.8 %) show a very large, and CI (−5.4 %) and NE (−3.3 %) exhibit a marked decline in EPE. Likewise, the largest reduction in CUE is observed in WGP (−6 %) and EH (−4.4 %). This is due to enhanced moisture stress and increased wildfires in the warmer and drier climate. NRA in the changes also reveal similar results, with the largest EPE (−4 %) decline among the bioclimatic regions in EH due to a substantial increase in aridity [CWD (18 %), VPD (3.3 %)], warming (T, 0.9 %) and drying [SM (−2.7 %), P (−0.16 %)]. WGP also exhibits a marked decline in EPE (−3 % NRA) due to predominant P drying (−5.8 %), SM stress (−0.63 %) and enhanced atmospheric aridity (VPD, 3 %) (Fig. S10).

4.4. Forest health: Sensitivity and Resilience

To understand impact of these changes and the ability of the forests to maintain their health, we estimate the sensitivity of EPE to its drivers (Fig. 2d). EPE exhibits very high negative sensitivity to T (−41) and VPD (−13), but low sensitivity to FPAR (−2.2), CWD (−0.63) and wildfires (−0.59). Conversely, EPE has positive sensitivity to moisture availability [(P, 4.5) and (SM, 2.3)]. CUE and WUE also exhibit similar sensitivities to their drivers but of a smaller magnitude (Fig. S11). On regional scale, both EPE and CUE shows very high negative sensitivity to T in WGP (−66, −48.3), IGP (−60.5, −28.5) and NE (−22.4, −19.4). Interestingly, CUE (16.5) and EPE (9.6) exhibit high positive sensitivity to T, but WUE shows high negative (−13.7) sensitivity to T in WH. Except in WGP, WUE has positive sensitivity to both VPD (7.7) and CWD (5.9), which is

highest in CI (Figs. 2d and S11).

Furthermore, the forest resilience to the moisture deficit (P, SM), warming (T), aridity (CWD, VPD) and wildfire (FC) are shown in Fig. 4. We find forests in most of lower WH, some areas in EH, NE and most of CI are non-resilient to P deficit (Fig. 4a). Likewise, forest ecosystems in most areas of WH, NE and CI are non-resilient to SM drying (Fig. 4b). Majority of forest ecosystems in WH, CI and some areas in EH and WGP are non-resilient to CWD (Fig. 4c). Likewise, there are regions such as WH, eastern CI, IGP and some areas in EH and NE, where forests are non-resilient to VPD stress (Fig. 4d). Forests in most of EH, WGP, some areas in NE and WH are non-resilient to warming (Fig. 4e). The forests non-resilient to wildfires are largely in EH, WG and some areas in WH and CI (Fig. 4f). The Indian forests are vulnerable to these extremes in various regions.

4.5. Forest health: Human influence and Integrity

The forests are not just impacted by climate change but also by human activities. To find the extend of human intervention on forests, we consider two indices, HMI and FLII, (Fig. 5). The forests in most of lower WH, IGP and WGP exhibit higher (0.35–0.6), and EH and lower NE exhibit lower human modifications (HMI < 0.25) (Fig. 5a). In India, most (56.34 % area) forests show moderate (8–9.6) and some (27.43 % area) in NE and CI exhibit low (0–6) integrity (FLII) (Fig. 5b). Conversely, some (16.22 % area) forests in EH and CI exhibit high (9.6–10) integrity. On regional scale, forests in EH has the smallest modifications (HMI=0.16) and thus exhibits largest integrity (FLII=8.2), but forests in CI exhibit high modifications (HMI=0.4) and low integrity (FLII=5.5). Likewise, forests in IGP exhibits lowest

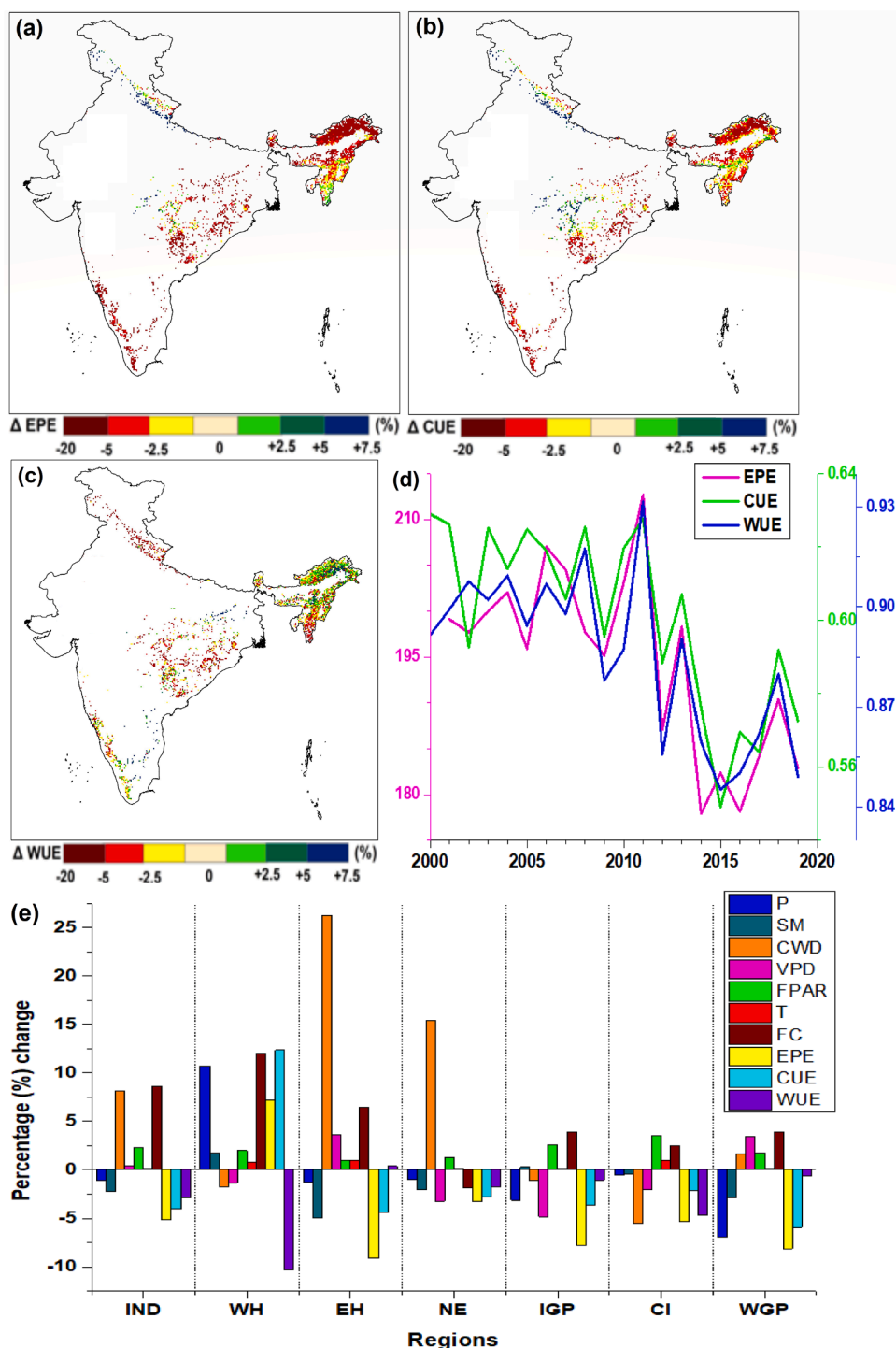


Fig. 3. Change (%) in (a) Ecosystem Photosynthetic Efficiency (EPE), (b) Carbon Use Efficiency (CUE) and (c) Water Use Efficiency (WUE) in recent decade (2010–2019) from the previous decade (2000–2009), (d) Temporal evolution in EPE, CUE and WUE during the period 2000–2019, (e) Percentage change in EPE, CUE, WUE and their divers- Precipitation (P), Soil Moisture (SM), Temperature (T), Climatic Water Deficit (CWD), Vapour Pressure Deficit (VPD), Fraction of Photosynthetically Active Radiation (FPAR), Vegetation Continuous Fields (VCF) and Fire Counts (FC) in recent decade (2010–2019) from the previous decade (2000–2009) for various regions in India (IND), and Western Himalaya (WH), Eastern Himalaya (EH), North East (NE), Indo-Gangetic Plain (IGP) Central India (CI) and Western Ghats and Peninsula (WGP).

integrity (FLII= 3.9) and large modifications (HMI=0.38). This hints at potential forest fragmentation by humans with hotspots in IGP and CI. Interestingly, despite high modifications (HMI= 0.37), forests in WH exhibits large (FLII= 7.7) integrity, which is opposite in the forests of NE (FLII= 6.2 and HMI= 0.28) (Fig. 5c, d). Furthermore, we also find a substantial increase in human population in the Indian forests during the

period 2000–2019. The forests in HR, NE, IGP, CI and WGP exhibit a huge population explosion (40–60 %) (Fig. S12). These regions are also the hotspots of human modification and forest fragmentation (Figs. 5 and S12).

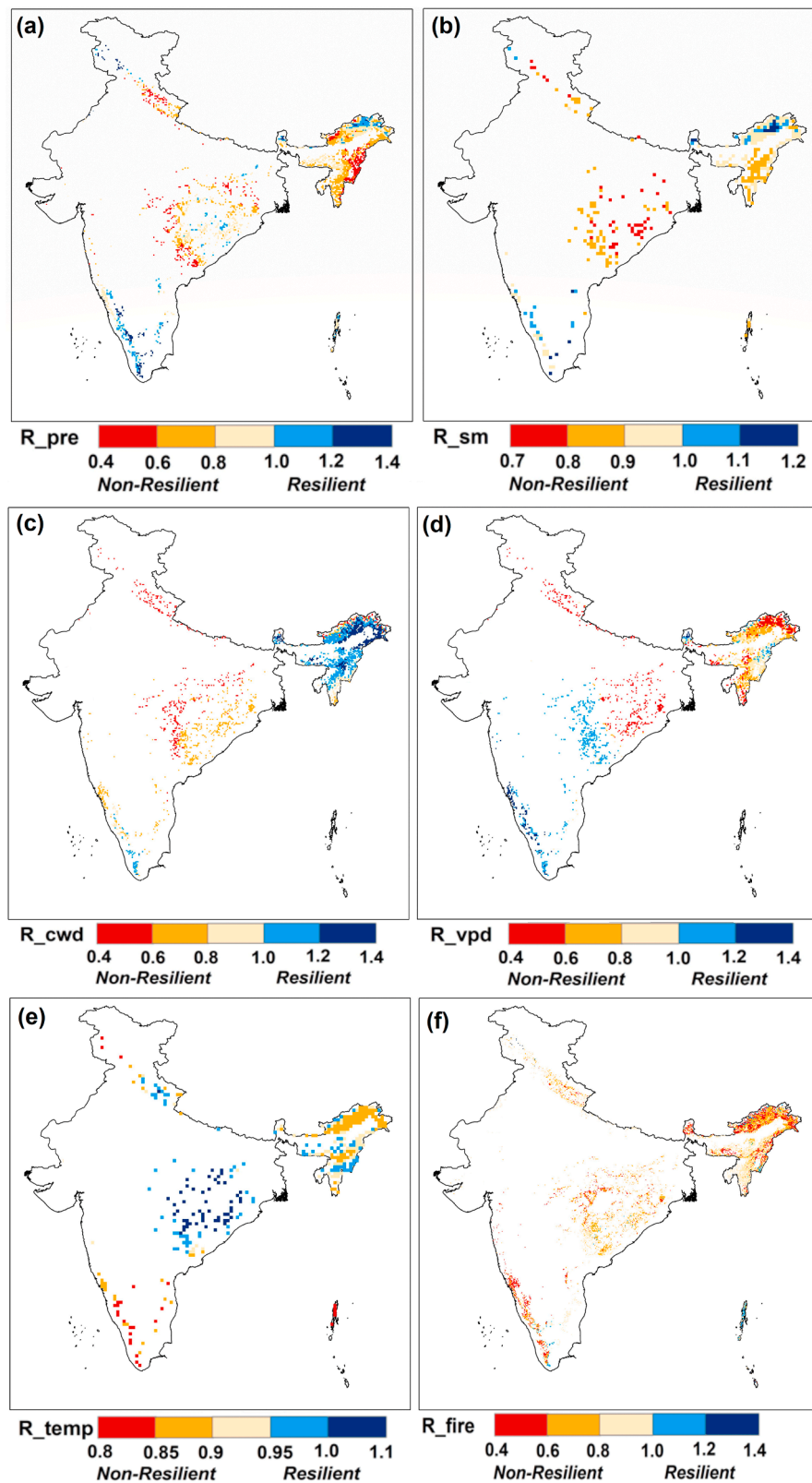


Fig. 4. Forest Resilience (R) to (a) Precipitation (R_{pre}) drying, (b) Soil Moisture stress (R_{sm}), (c) land evaporative aridity (R_{cwd}), (d) atmospheric aridity (R_{vpd}), (e) warming (R_{temp}) and (f) wildfires (R_{fire}) during the period 2000–2019.

4.6. Forest health: Growth Rate, age and the future

The Growth Rate (GR) analysis during the period 2000–2019 reveals greening of Indian forests with positive CGR in NDVI (2.7%), VCF (2%),

LAI (7.4%) and SIF (6.1%). However, this greening is not being efficiently translated in carbon uptake as exhibited by the negative CGR in NPP (−3.54%) and a reduction in translation of greenness to carbon uptake (EPE, −2.67%), which substantially deteriorates forest health

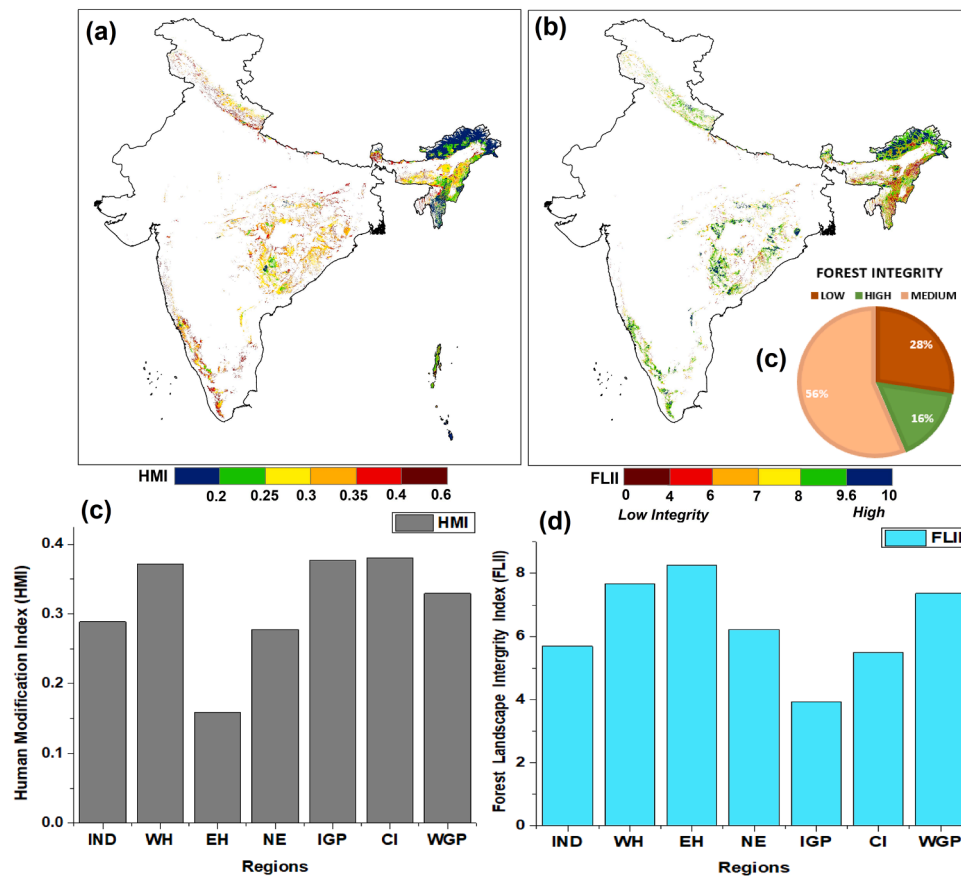


Fig. 5. (a) Human Modification Index (HMI), (b) Forest Landscape Integrity Index (FLII), and (c) area (%) in various FLII categories (low, medium and high forest integrity), and (d) HMI and (e) FLII for India (IND), and Western Himalaya (WH), Eastern Himalaya (EH), North East (NE), Indo-Gangetic Plain (IGP) Central India (CI) and Western Ghats and Peninsula (WGP).

[negative CGR in CUE (−10.75 %) and WUE (−5.8 %) in India. This is driven by positive CGR in aridity [VPD (9.9 %), CWD (5.1 %)], T (2.26 %) and wildfires (12.34 %), and negative CGR in moisture availability [SM (−2.47 %), P (−2.1 %)] as depicted in Fig. 6b. Apart from the climate drivers, there are human interventions that negatively impact the forest structure and functioning. To closely examine this, we analyse the forest age (Fig. 6a) and forest loss (Fig. S13) in India. We find that most forests in India are middle aged (30–60 years), and are mainly found in the foothills of WH, most of EH, NE, CI and northern WGP. The forests in India are young (< 30 years) in the regions of southern WGP, eastern CI, and IGP. In contrast, old age (60–150 years) forests are predominantly found in the Himalaya (northern WH and EH). We find forest loss as the conversion of forests to non-forest lands during the period from 2001 to 2019, primarily in CI (23 % NRA) and WGP (10 % NRA). This explains the decline in EPE in Indian forests with its peak in the pristine forests of EH and WGP. Thus, we find declining forest carbon sink potential in India despite greening due to both changing climate and anthropogenic intrusions. Henceforth, the future fate of forest carbon stocks in India in this scenario needs to be explored.

In order to investigate the future of forest ecosystems in India, we employ CMIP6 future projections and LPJ-GUESS process-based ecosystem model results. From the CMIP6 (Fig. S14), we find increase in all parameters except CUE (−0.6 %) in the end of the century (P3, 2090–2100) from the base period (P1, 2015–2019). Furthermore, we split the time span into two focal periods, i.e., F1 is mid-century (P2, 2040–2050) from the base period (P1, 2015–2019); and F2 is end-century (P3) from P2. We find large increase in all parameters in F1 wherein, greenness (LAI, 6 %), carbon uptake (NPP, 23 %) and conversion (EPE, 8.6 %) are prominent. In F2, there is smaller increase in

NPP (10.7 %) despite larger increase in LAI (14 %) due to reduction in EPE (−1.35 %). Among the two focal periods (Fig. 6c), there is predominant decline in carbon uptake (−12.3 %), despite greening (8.2 %) due to decline in EPE (−10 %). The decrease in EPE also degrades forest health (CUE, −3.8 %) and (WUE, −5 %).

We run the LPJ-GUESS DGVM, for examining the effect of climate change on forests. Therefore, the model is run for both no-climate change (Fig. S15), and climate change scenarios (Fig. 6d). In no-climate change scenario, there are very small and inconsistent changes among the parameters in the period (P3-P1). In contrast, we find increase in all parameters (LAI, NPP, biomass and leaf C:N) in the period (P3-P1) in the climate change scenario. As done before, we split the time span into two focal periods (F1 and F2) for detailed investigation. Interestingly, there is a substantial increase in each parameter [(LAI, 10.6 %), (NPP, 14.2 %), (biomass, 20 %) and (leaf C:N, 10.4 %)] in F1. However, there is decline in each parameter [(LAI, −3.7 %), (NPP, −0.9 %), (biomass, 20 %) and (leaf C:N, 10.4 %)] in F2 (Fig. S14). Between the two focal periods (F1 and F2), there is a substantial decline in all parameters such as greenness (−14.3 %), carbon uptake (−15 %), biomass (−23.2 %) and leaf C:N (−13.8 %) in the climate change context. Contrarily, in no-climate change scenario, there are very small changes in all parameters, where carbon uptake has smaller decline than in the climate change run (Fig. 6d). Therefore, both LPJ DGVM results and CMIP6 future projections reveal that the strength of Indian forest carbon sinks is declining in the future.

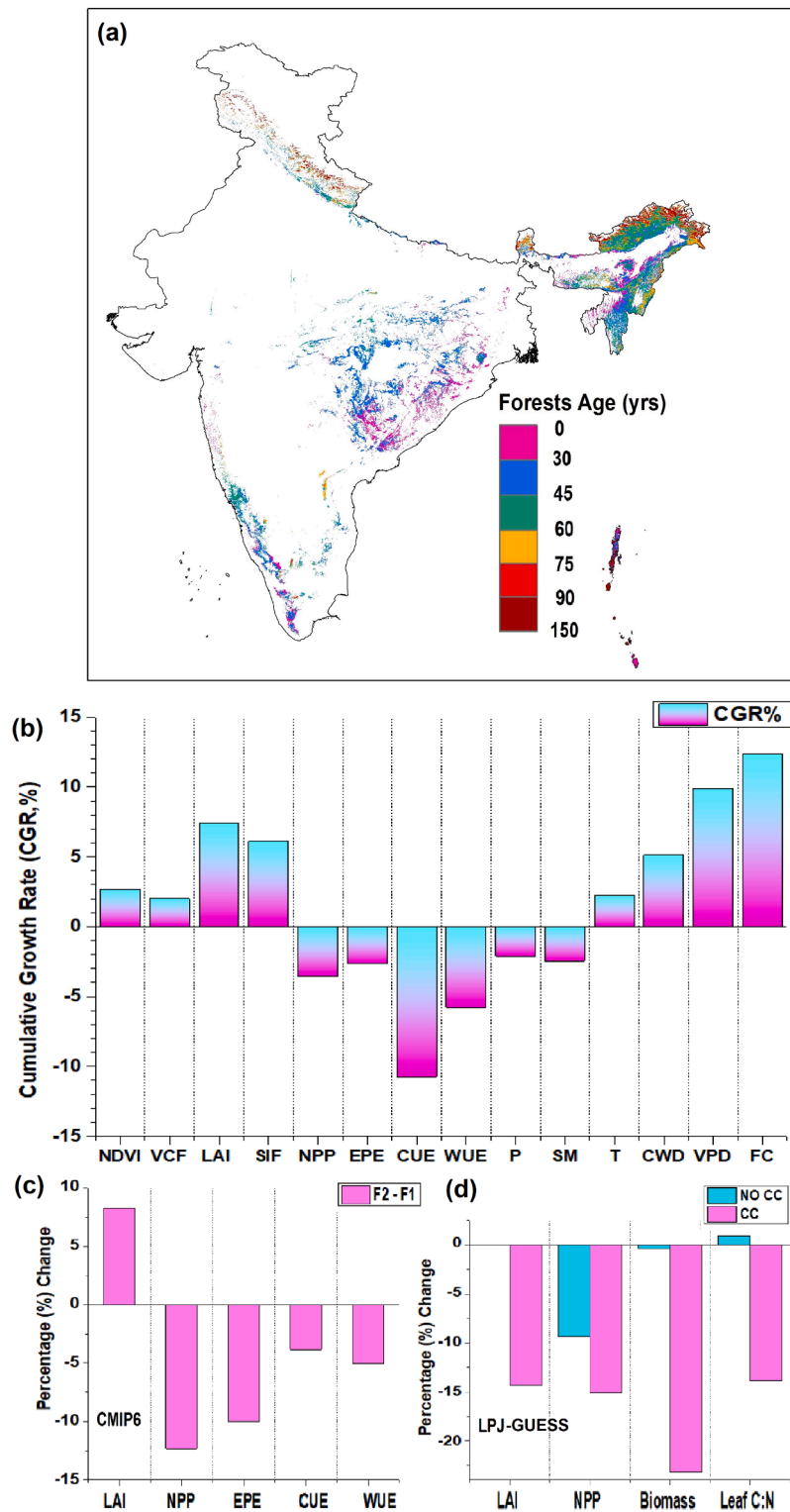


Fig. 6. (a) Forest Age (in years) in the year 2010, (b) Cumulative Growth Rate in vegetation greenness and photosynthesis [(Normalised Difference Vegetation Index: NDVI), (Vegetation Continuous Fields: VCF), (Leaf Area Index: LAI) and (Solar-Induced Fluorescence: SIF)], functioning and health [(Net Primary Productivity: NPP), (Ecosystem Photosynthetic Efficiency: EPE), (Carbon Use Efficiency: CUE) and (Water Use Efficiency: WUE)] and their climate drivers [(Precipitation: P), (Soil Moisture: SM), (Temperature: T), (Climatic Water Deficit: CWD), (Vapour Pressure Deficit: VPD) and (Fire Counts: FC)] for the period 2000–2019. Percentage (%) change in (c) greenness (LAI), carbon uptake (NPP), EPE, CUE and WUE from the CMIP6 model results, (d) LAI, NPP, and biomass and leaf carbon:nitrogen ratio (Leaf C:N) from the LPJ-GUESS model simulations between mid-century (P2, 2040–2050) to end-century (P3, 2090–2100) i.e. focal period 2 (F2) from mid-century to base period (P1, 2015–2019) i.e. focal period 1 (F1) in no climate change (NO CC) and climate change (CC) runs.

5. Discussion

5.1. Indian forest carbon stocks: significance

The global atmospheric CO₂ and average temperature have risen substantially since the industrial revolution (IPCC, 2021; Friedlingstein et al., 2024). India is no different, as the CO₂ concentration in India has been increasing rapidly (2.1 ppm/yr) over the past few decades (2002–2020) similar to those in the global tropical and mid-latitudes (Kuttippurath et al., 2022). This increase in atmospheric CO₂ in India can be attributed to anthropogenic emissions, agricultural and soil emissions, and inadequate land management practices (Singh et al., 2022). Since the Kyoto Protocol (1997), there has been a notable emphasis on forests for the purpose of carbon sequestration and mitigation of global warming (IPCC, 2021; Friedlingstein et al., 2024). Under the Bonn Challenge (2011) and Land Degradation Neutrality (LDN) goals (2015), India is committed to restore 26 million hectares of degraded land by 2030. Also, maintaining forest carbon sinks and their resilience to climate change and human interventions is key to attain India's target of net zero emissions by 2070 (ISFR, 2021, 2023). South Asia continues to be a carbon sink with India being the largest contributor, both as a source and a sink (Jain et al., 2025). However, despite lying in the tropical region of higher carbon uptake, the fate of forest carbon stocks in the current and future climate change scenarios is largely underexplored for India, and therefore, this is the first comprehensive study in this regard.

5.2. Mismatch between forest greening and carbon uptake

We find that there is greening of Indian forests in terms of increase in greenness and photosynthesis (FPAR, LAI and SIF) consistent with our previous finding Kuttippurath and Kashyap (2023). The Indian forests are greening in recent decades due to several land development initiatives such as the National Afforestation Programme (NAP) and Green India Mission (GIM) implemented by the Ministry of Environment, Forest and Climate Change (MoEFCC) focused on plantations and afforestation drives (ISFR, 2021, 2023; Pasha and Dadhwal, 2024). However, there is a decline in forest carbon uptake (NPP) of Indian forests despite greening. The limited cropland canopy carbon uptake and low GPP in forests resulted in weak carbon uptake in India during recent decades (Sarmah et al., 2021). Interestingly, there is a mismatch between the greening and carbon sink potential in India (Kashyap et al., 2023a). A recent study also finds this inability of translation of greenness to productivity in major forests of India due to warming. It states that, above a threshold temperature, GPP decreases and wherein respiration becomes stable and reduce NPP (Das et al., 2023). Apart from warming, there must be other ecosystem processes and certain biophysical mechanisms that inhibits the carbon uptake despite increased greenness in Indian forests.

5.3. Declining forest carbon stocks: Climate change and anthropogenic intrusions

To further investigate this, we estimate EPE (translation of greenness to carbon uptake) for the first time for Indian forests and find that EPE has declined substantially in recent decade (2010–2019) from the previous (2000–2009). Interestingly, the largest decline in EPE is for the pristine forests of EH, WGP and IGP which also have the highest EPE. This explains the hindered ability of Indian forests to translate greenness to carbon uptake during recent decade. In addition, declining EPE adversely impacts the forest health with reduction in CUE and WUE, predominant in the pristine forests of WGP and EH. The decline in forest ecosystem health can be attributed to the reduced moisture availability, increased aridity, enhanced warming and frequent wildfires in recent decade (2010–2019). Correlation analysis and Granger Causality test reveal SM and T as the key drivers of EPE. We also find SM (26.7 %) to

have a stronger control on EPE than T (13.2 %) for the Indian forests, as per RF analysis. The forest health metrics (EPE, CUE and WUE) exhibit higher negative sensitivity to T and VPD, low negative sensitivity to FPAR, CWD and wildfires, and positive sensitivity to P and SM. Interestingly, the sensitivity of EPE to its drivers surpasses that of CUE and WUE. Rising moisture stress and intense warming adversely affect the health and functioning of terrestrial ecosystems in India (Das et al., 2023; Kashyap and Kuttippurath, 2024a, b). Accelerated warming and wildfires have depleted the forests and negatively impacted the carbon sinks in recent decades (Haughan et al., 2022) in India, particularly with wildfire hotspots in WH, EH and CI (Sannigrahi et al., 2020), and more frequent fires are expected in the warmer and drier future climate (Bar et al., 2024). Frequent landslides in the Himalayan region can also deplete the carbon sinks (Kashyap et al., 2021). The forests are non-resilient to moisture stress, aridity, warming and wildfires, with hotspots in the pristine forests of EH and WGP.

Furthermore, there are noticeable human modifications leading to forest fragmentation (loss of integrity) with hotspots in IGP and CI. Nevertheless, some forests (16.2 % area) in India have high forest integrity, though much lower than the global average of 40 % (Grantham et al., 2020). We find young forests (< 30 years) in the regions of predominant forest loss in CI and WGP. Also, there has been a substantial decline in the large and mature trees in India, which are replaced with small plantations in recent decade (Brandt et al., 2024). The large-scale anthropogenic intrusions such as deforestation owing to the traditional agricultural practices (slash and burn, and shifting jhum cultivation) (Sparsha and Parida, 2024), plantation expansion, encroachment, mining activities and other developmental activities have led to forest degradation in the ecologically sensitive regions of EH, NE, CI and WG (Reddy et al., 2018; ISFR, 2023). Since 2012, the Western Ghats are designated as the UNESCO World Heritage site for being one of the planet's most biologically diverse hotspots, but the region experienced 7 % deforestation during 2001–2020 (Pasha and Dadhwal, 2024) with a notable decline in moderately dense and open forests (ISFR, 2023). Concurrently, there is an increase in plantation trees outside the forests and savanna in India (ISFR, 2023; Pasha and Dadhwal, 2024).

5.4. Future of forest carbon stocks: Implications and Recommendations

From the CMIP6 model results we find a marked decline in carbon uptake (NPP, –12.3 %), despite greening (LAI, +8.2 %) in Indian forests between mid-century (2040–2050) to end-century (2090–2100) from mid-century to base period (2015–2019). This is due to the reduction in translation of greenness to carbon uptake (EPE, –10 %) that leads to reduced carbon (CUE, –3.8 %) and water (WUE, –5 %) sequestration of the forests while maintaining carbon uptake. Likewise, the results from a process-based DGVM in LPJ-GUESS exhibit a substantial decline in carbon uptake (–15 %), biomass (–23.2 %) and leaf C:N (–13.8 %) during the same period. This indicates the weakening of the forest carbon sinks and declining forest health is likely to be stronger in the future due to climate change and anthropogenic interventions in India. A recent study also finds a declining NPP growth rate from 2021 to 2099 for the Indian terrestrial ecosystems and attributes it to weakening CO₂ fertilization effect (CFE) (Bejagam et al., 2024). This is in coherence with the limited and reduced CFE due to rising nutrient and water limitations in the current and future climate (Wang et al., 2020; Winkler et al., 2021). Additionally, the radiative effects of increasing CO₂ as a potent greenhouse gas (GHG) would drive unprecedented warming and counterbalance the fertilization effects (Peñuelas et al., 2017; Shi et al., 2021).

The degradation of forest resources is a concern for the economy of a country and would eventually impact its timber production, market price, planting intensity and lives of forest dwellers in India. Additionally, it threatens the indigenous biodiversity and pushes them towards extinction. Also, degradation of forests in ecologically fragile regions like EH, NE and WG can lead to more frequent climatic extremes in the

future. Furthermore, forests possess a restricted capacity for carbon storage, which is insufficient to effectively address the rise in atmospheric CO₂. Furthermore, a substantial part of carbon is stored in non-living systems on land (Bar-On et al., 2025). Henceforth, it is imperative to avoid misconstruing forest-based climate mitigation as a solution to current anthropogenic carbon emissions levels (Canadell, 2025). The ageing tropical forests might get saturated as carbon sinks in the future (Yang et al., 2023; Wigner et al., 2024). Conversely, endeavours to counteract deforestation and enhance carbon reserves should be promoted as valuable and efficient approaches to counterbalance the residual emissions to achieve the target of net-zero emissions by 2070 in India. Henceforth, there is a need for better management of land-based carbon emissions and advanced technologies for carbon capture and sequestration. Additionally, the afforestation programmes should be more scientific and focused on maintaining the existing forest areas, including the historical natural forests. Furthermore, studies on forest carbon dynamics should be encouraged for the Indian region integrating remote sensing observations and ground-based measurements.

5.5. Limitations

The study employs remote sensing measurements, which have uncertainties such as saturation and insufficient sensitivity in the dense canopy regions. There is a severe lack of ground-based measurements for the estimation of carbon and water fluxes for the Indian region. Therefore, satellite data with higher resolution and more surface measurements would improve our understanding of Indian forest carbon dynamics. The CMIP6 model results are subject to limitations like insensitive to efficiently account for dryness stress such as SM, VPD and compound SM-VPD stresses on vegetation (Liu et al., 2023; Song et al., 2024) and they overestimate the future greening (Wu et al., 2022). The CMIP6 models are also subject to limited ability to simulate the extreme events such as mega-droughts, heatwaves, intense wildfires, human mismanagements, destructive logging, insect and disease outbreaks, and forest diebacks (Zhao et al., 2020; Wu et al., 2022). These models also face challenges in simulating the influence of climate oscillations like El Niño Southern Oscillation (ENSO), which substantially impact photosynthesis (Kashyap and Kuttippurath, 2025) and carbon stocks (Wigner et al., 2020) in the tropical regions of higher carbon uptake. In addition, the CMIP6 model results are constrained by coarse resolution and thus, it affects the accuracy of simulations on regional scales. Process-based ecosystems models like LPJ-GUESS are originally calibrated for global climate regions and henceforth, they might not very efficiently capture regional variability, particularly for a very complex vegetation-climate-human interaction landscape like India. The statistical and ML techniques employed in this study are subject to some limitations as they are largely data-driven, which demand more measurements to produce robust results. The natural variability in forests such as succession, defoliation, regeneration, changes in soil composition, altered nutrient cycle and plant species distribution are very complex and are not accounted for in these analyses, which could also add some uncertainty in the results. The study period is based on the availability of data post-MODIS era (since 2000), and the years post-2019 such as 2020 and 2021 are not considered as they exhibit high anomalies due to the impact of COVID-19 lockdown (Kashyap et al., 2023b).

6. Conclusions

Forests are major carbon sinks and are considered as nature-based solutions (NbS) to combat climate change. We, for the first time, thoroughly investigate the structure (greenness), functioning (carbon uptake), translation of greenness to carbon uptake (EPE), health (CUE and WUE), climate and anthropogenic drivers of change, and spatio-temporal evolution in the current and future climate scenarios for the Indian forests. We employ a suite of statistical and ML techniques on a

range of remote sensing, reanalysis, the CMIP6 model projections and the LPJ-GUESS process based vegetation model data. We find limited ability of Indian forest ecosystems to translate the greenness to carbon uptake in recent decades (2000–2019). Previous studies have reported mismatch between greening and carbon uptake and hindered translation of greening to enhanced carbon uptake in India and attributed it the impacts of climate change driven warming. However, we compute a novel metric—the Ecosystem Photosynthetic Efficiency (EPE) to explicitly explain the inhibited translation of the structure and functioning of Indian forests. We find substantial decline in EPE during recent decade (2010–2019) from the previous decade (2000–2009), predominant in the hotspots of highest EPE such as EH, WGP and IGP. The decrease in EPE also drives reduction in CUE and WUE of the forests. Our analysis finds that the decline in forest health and functioning (EPE, CUE and WUE) is due to enhanced moisture stress, rising aridity and increased wildfires, in addition to rapid surface warming. Forest health and functioning exhibit high negative sensitivity to T and VPD, low negative sensitivity to FPAR, CWD and wildfires, and high positive sensitivity to moisture availability (P and SM). Forests ecosystems are non-resilient to drying, aridity, warming and frequent wildfires in most regions, with the pristine forests in EH and WGP being the hotspots. Additionally, human-driven modifications have led to loss of forest integrity, with IGP and CI as its hotspots. Both CMIP6 projections and process based DGVM in LPJ-GUESS results reveal that there is a notable decrease in the carbon uptake, despite greening due to the decline in EPE, which reduces CUE and WUE between mid-century (2040–2050) to end-century (2090–2100) from mid-century to the historical period (2015–2019). This suggests that the forest carbon sinks in India are weakening under the current and future climate change scenarios.

The study has some limitations due to the uncertainties in the remote sensing, reanalyses, and the model data. The lack of ground-based data in India and limitations of the statistical and ML methods adds to these uncertainties. Therefore, these findings call for establishment of an efficient network of ground-based stations in the Indian region, as its forests are weakening as carbon sinks, home to rich biodiversity and support food and livelihood of billions in the country. Future studies should integrate remote sensing data with in-situ measurements with a focus on the ecologically fragile and climate extreme prone pristine forests of Himalaya and Western Ghats. In the future, accelerated deforestation and forest degradation due to changing climate, rising extremes, agricultural expansion, plantation growth and rapid developmental activities can lead to savannisation of Indian forests. Henceforth, there is an urgent need for preservation of indigenous forests, sustainable and judicious use of forest resources, improved forest management practices, scientific afforestation programmes, substantial reduction in carbon emissions and better carbon capture technologies to achieve sustainability and the target of net zero emissions in India by the year 2070.

CRedit authorship contribution statement

Rahul Kashyap: Writing – review & editing, Writing – original draft, Visualization, Software, Methodology, Formal analysis, Data curation, Conceptualization, Investigation. **Jayanarayanan Kuttippurath:** Writing – review & editing, Visualization, Supervision, Resources, Methodology, Conceptualization.

Declaration of competing interest

The authors declare that they have no known competing financial interests or personal relationships that could have appeared to influence the work reported in this paper.

Acknowledgments

We thank the Director, Indian Institute of Technology Kharagpur (IIT

Kgp), Chairman of CORAL IIT Kgp and the Ministry of Education (MoE) for facilitating the study. RK acknowledges the support from Prime Minister's Research Fellowship (PMRF), MoE. We thank all the data providing sources like NASA's LPDAAC team for providing the MODIS land cover, NDVI, LAI, GPP, NPP, ET, ASTER DEM and VCF products. We also thank Giovanni's online data system, developed and maintained by the NASA GES DISC, for providing the GPM level-3 precipitation data; GLDAS for providing SM datasets; ERA-5 for air temperature data; TerraClimate for CWD and VPD datasets; SEDAC for HMI data; GFW for canopy cover data; GlobBiomass for AGB data; CMIP6 for providing future projections; WorldPop for population data, MPI-BGC for forest age data. We also sincerely thank the team that developed LPJ-GUESS DVGM. Special thanks to Jingfeng Xiao for SIF, and Hedley Grantham for making FLII datasets as available publicly.

Supplementary materials

Supplementary material associated with this article can be found, in the online version, at [doi:10.1016/j.resconrec.2025.108478](https://doi.org/10.1016/j.resconrec.2025.108478).

Data availability

All data are publicly available, and listed in Table S1.

References

- Bar, S., Acharya, P., Parida, B.R., Sannigrahi, S., Maiti, A., Barik, G., Kumar, N., 2024. Investigation of fire regime dynamics and modeling of burn area over India for the twenty-first century. *Environ. Sci. Pollut. Res.* 31 (41), 53839–53855. <https://doi.org/10.1007/s11356-024-32922-w>.
- Bar-On, Y.M., Li, X., O'Sullivan, M., Wigneron, J.P., Sitch, S., Ciais, P., Fischer, W.W., et al., 2025. Recent gains in global terrestrial carbon stocks are mostly stored in nonliving pools. *Science* (1979) 387 (6740), 1291–1295. <https://doi.org/10.1126/science.adk1637>.
- Bauman, D., Fortunel, C., Delhaye, G., Malhi, Y., Cernusak, L.A., Bentley, L.P., McMahon, S.M., et al., 2022. Tropical tree mortality has increased with rising atmospheric water stress. *Nature* 608 (7923), 528–533. <https://doi.org/10.1038/s41586-022-04737-7>.
- Bejagam, V., Sharma, A., Wei, X., 2024. Projected decline in the strength of vegetation carbon sequestration under climate change in India. *Sci. Total Environ.* 916, 170166. <https://doi.org/10.1016/j.scitotenv.2024.170166>.
- Besnard, S., Koirala, S., Santoro, M., Weber, U., Nelson, J., Gütter, J., Carvalhais, N., et al., 2021. Mapping global forest age from forest inventories, biomass and climate data. *Earth Syst. Sci. Data Discuss.* 2021, 1–22. <https://doi.org/10.5194/essd-13-4881-2021>.
- Brandt, M., Gominski, D., Reiner, F., Kariyaa, A., Guthula, V.B., Ciais, P., Fensholt, R., et al., 2024. Severe decline in large farmland trees in India over the past decade. *Nat. Sustain.* 7 (7), 860–868. <https://doi.org/10.1038/s41893-024-01356-0>.
- Breiman, L., 2001. Random forests. *Mach. Learn.* 45, 5–32. <https://doi.org/10.1023/A:1010933404324>.
- Canadell, J.G., 2025. Looking beyond the trees for carbon storage. *Science* (1979) 387 (6740), 1252–1253. <https://doi.org/10.1126/science.adw3259>.
- Chen, C., Park, T., Wang, X., Piao, S., Xu, B., Chaturvedi, R.K., Myneni, R.B., et al., 2019. China and India lead in greening of the world through land-use management. *Nat. Sustain.* 2 (2), 122–129. <https://doi.org/10.1038/s41893-019-0220-7>.
- Crowther, T.W., Glick, H.B., Covey, K.R., Bettigole, C., Maynard, D.S., Thomas, S.M., Bradford, M.A., et al., 2015. Mapping tree density at a global scale. *Nature* 525 (7568), 201–205. <https://doi.org/10.1038/nature14967>.
- Das, R., Chaturvedi, R.K., Roy, A., Karmakar, S., Ghosh, S., 2023. Warming inhibits increases in vegetation net primary productivity despite greening in India. *Sci. Rep.* 13 (1), 21309. <https://doi.org/10.1038/s41598-023-48614-3>.
- Farr, T.G., Rosen, P.A., Caro, E., Crippen, R., Duren, R., Hensley, S., Alsdorf, D., et al., 2007. The shuttle radar topography mission. *Rev. Geophys.* 45 (2). <https://doi.org/10.1029/2005RG000183>.
- Feng, Y., Ciais, P., Wigneron, J.P., Xu, Y., Ziegler, A.D., van Wees, D., Zeng, Z., et al., 2024. Global patterns and drivers of tropical aboveground carbon changes. *Nat. Clim. Chang.* 14 (10), 1064–1070. <https://doi.org/10.1038/s41558-024-02115-x>.
- Friedlingstein, P., O'Sullivan, M., Jones, M.W., Andrew, R.M., Hauck, J., Landschützer, P., Zeng, J., et al., 2024. Global carbon budget 2024. *Earth Syst. Sci. Data Discuss.* 2024, 1–133. <https://doi.org/10.5194/essd-17-965-2025>.
- Gang, C., Wang, Z., You, Y., Liu, Y., Xu, R., Bian, Z., Zhang, M., et al., 2022. Divergent responses of terrestrial carbon use efficiency to climate variation from 2000 to 2018. *Glob. Planet. Change* 208, 103709. <https://doi.org/10.1016/j.gloplacha.2021.103709>.
- Giglio, L., Schroeder, W., Justice, C.O., 2016. The collection 6 MODIS active fire detection algorithm and fire products. *Remote Sens. Environ.* 178, 31–41. <https://doi.org/10.1016/j.rse.2016.02.054>.
- Granger, C.W., 1969. Investigating causal relations by econometric models and cross-spectral methods. *Econometr. J. Econometr. Soc.* 424–438. <https://www.jstor.org/stable/1912791>.
- Grantham, H.S., Duncan, A., Evans, T.D., Jones, K.R., Beyer, H.L., Schuster, R., Watson, J.E.M., et al., 2020. Anthropogenic modification of forests means only 40% of remaining forests have high ecosystem integrity. *Nat. Commun.* 11 (1), 5978. <https://doi.org/10.1038/s41467-020-19493-3>.
- Harris, N., Gibbs, D., 2021. Forests absorb twice as much carbon as they emit each year. *World Resour. Inst. (WRI) Insights.* January 21. <https://www.wri.org/insights/forests-absorb-twice-much-carbon-they-emit-each-year>.
- Haughan, A.E., Petteorelli, N., Potts, S.G., Senapathi, D., 2022. The role of climate in past forest loss in an ecologically important region of South Asia. *Glob. Chang. Biol.* 28 (12), 3883–3901. <https://doi.org/10.1111/gcb.16161>.
- Holling, C.S., 1973. Resilience and stability of ecological systems. *Annu. Rev. Ecol. Syst.* 4 (1), 1–23. <https://doi.org/10.1017/9781009177856.038>.
- Huang, M., Zhai, P., Piao, S., 2021. Divergent responses of ecosystem water use efficiency to drought timing over Northern Eurasia. *Environ. Res. Lett.* 16 (4), 045016. <https://doi.org/10.1088/1748-9326/abf0d1>.
- Humphrey, V., Berg, A., Ciais, P., Gentile, P., Jung, M., Reichstein, M., Frankenberg, C., et al., 2021. Soil moisture–atmosphere feedback dominates land carbon uptake variability. *Nature* 592 (7852), 65–69. <https://doi.org/10.1038/s41586-021-03325-5>.
- IPCC, 2021. *Climate change 2021: the physical science basis. Contribution of Working Group I to the 6th Assessment Report of the Intergovernmental Panel on Climate Change.* Cambridge Press, Cambridge, UK.
- ISFR, 2021. *India State of the Forest Report. Forest Survey of India, The Ministry of Environment, Forest and Climate Change (MoEFCC). Govt. of India, Dehradun.* <https://fsi.nic.in/forest-report-2021>.
- ISFR, 2023. *India State of the Forest Report. Forest Survey of India, The Ministry of Environment, Forest and Climate Change (MoEFCC). Govt. of India, Dehradun.* https://fsi.nic.in/uploads/isfr2023/isfr_book_eng-vol-1_2023.pdf.
- Jain, A.K., Seshadri, S., Anand, J., Chandra, N., Patra, P.K., Canadell, J.G., Tiwari, Y.K., et al., 2025. South Asia's ecosystems are a net carbon sink, but the region is a major net GHG source to the atmosphere. *Glob. Biogeochem. Cycles* 39 (4). <https://doi.org/10.1029/2024GB008261>.
- Kashyap, R., Pandey, A.C., 2021. Spatio-temporal variability assessment of pre-monsoon temperature to deduce their impact on Forest Fire events in relation to relief across Himalayan region. *J. Geomat.* 15 (2), 106–114. <https://isgindia.org/volume-15-no-2-october-2021>.
- Kashyap, R., Kuttippurath, J., Patel, V.K., 2025. Agriculture intensification and moisture-induced Thar desert greening: implications for energy balance, socio-economy, and biodiversity. *Gisci. Remote Sens.* 62 (1), 2483458. <https://doi.org/10.1080/15481603.2025.2483458>.
- Kashyap, R., Kuttippurath, J., 2025. Tropical cyclones enhance photosynthesis in moisture-stressed regions of India. *NPJ Clim. Atmos. Sci.* 8 (1), 115. <https://doi.org/10.1038/s41612-025-00988-z>.
- Kashyap, R., Kuttippurath, J., 2024a. Unraveling the sensitivity and response of ecosystems to rising moisture stress in India. *Ecosyst. Health Sustain.* 9, 0180. <https://doi.org/10.1016/j.jenvman.2023.117655>.
- Kashyap, R., Kuttippurath, J., 2024b. Warming-induced soil moisture stress threatens food security in India. *Environ. Sci. Pollut. Res.* 31 (49), 59202–59218. <https://doi.org/10.1007/s11356-024-35107-7>.
- Kashyap, R., Kuttippurath, J., Kumar, P., 2023a. Browning of vegetation in efficient carbon sink regions of India during the past two decades is driven by climate change and anthropogenic intrusions. *J. Environ. Manage.* 336, 117655. <https://doi.org/10.1016/j.jenvman.2023.117655>.
- Kashyap, R., Kuttippurath, J., Patel, V.K., 2023b. Improved air quality leads to enhanced vegetation growth during the COVID-19 lockdown in India. *Appl. Geogr.* 151, 102869. <https://doi.org/10.1016/j.apgeog.2022.102869>.
- Kashyap, R., Pandey, A.C., Kuttippurath, J., 2022. Photosynthetic trends in India derived from remote sensing measurements during 2000–2019: vegetation dynamics and key climate drivers. *Geocart. Int.* 37 (26), 11813–11829. <https://doi.org/10.1080/10106049.2022.2060325>.
- Kashyap, R., Pandey, A.C., Parida, B.R., 2021. Spatio-temporal variability of monsoon precipitation and their effect on precipitation triggered landslides in relation to relief in Himalayas. *Spat. Inf. Res.* 29 (6), 857–869. <https://doi.org/10.1007/s41324-021-00392-8>.
- Keenan, T.F., Hollinger, D.Y., Bohrer, G., Dragoni, D., Munger, J.W., Schmid, H.P., Richardson, A.D., 2013. Increase in forest water-use efficiency as atmospheric carbon dioxide concentrations rise. *Nature* 499 (7458), 324–327. <https://doi.org/10.1038/nature12291>.
- Keenan, T.F., Prentice, I.C., Canadell, J.G., Williams, C.A., Wang, H., Raupach, M., Collatz, G.J., 2016. Recent pause in the growth rate of atmospheric CO₂ due to enhanced terrestrial carbon uptake. *Nat. Commun.* 7 (1), 13428. <https://doi.org/10.1038/ncomms13428>.
- Kennedy, C.M., Oakleaf, J.R., Theobald, D.M., Baruch-Mordo, S., Kiesecker, J., 2019. Managing the middle: a shift in conservation priorities based on the global human modification gradient. *Glob. Chang. Biol.* 25 (3), 811–826. <https://doi.org/10.1111/gcb.14549>.
- Kong, X., Zhou, Z., Jiao, L., 2021. Hotspots of land-use change in global biodiversity hotspots. *Resour. Conserv. Recycl.* 174, 105770. <https://doi.org/10.1016/j.resconrec.2021.105770>.
- Kuttippurath, J., Kashyap, R., 2023. Greening of India: forests or croplands? *Appl. Geogr.* 161, 103115. <https://doi.org/10.1016/j.apgeog.2023.103115>.

- Kuttippurath, J., Peter, R., Singh, A., Raj, S., 2022. The increasing atmospheric CO₂ over India: comparison to global trends. *iScience* 25 (8). <https://doi.org/10.1016/j.isci.2022.104863>.
- Li, X., Xiao, J., 2019. Mapping photosynthesis solely from solar-induced chlorophyll fluorescence: a global, fine-resolution dataset of gross primary production derived from OCO-2. *Remote Sens.* 11 (21), 2563. <https://doi.org/10.3390/rs11212563> (Base).
- Liu, X., Sun, G., Fu, Z., Ciais, P., Feng, X., Li, J., Fu, B., 2023. Compound droughts slow down the greening of the Earth. *Glob. Chang. Biol.* 29 (11), 3072–3084. <https://doi.org/10.1111/gcb.16657>.
- MacBean, N., Maignan, F., Bacour, C., Lewis, P., Peylin, P., Guanter, L., Disney, M., et al., 2018. Strong constraint on modelled global carbon uptake using solar-induced chlorophyll fluorescence data. *Sci. Rep.* 8 (1), 1973. <https://doi.org/10.1038/s41598-018-20024-w>.
- Nemani, R.R., Keeling, C.D., Hashimoto, H., Jolly, W.M., Piper, S.C., Tucker, C.J., Running, S.W., et al., 2003. Climate-driven increases in global terrestrial net primary production from 1982 to 1999. *Science* (1979) 300 (5625), 1560–1563. <https://doi.org/10.1126/science.1082750>.
- Pan, Y., Birdsey, R.A., Phillips, O.L., Houghton, R.A., Fang, J., Kauppi, P.E., Murdiyarso, D., et al., 2024. The enduring world forest carbon sink. *Nature* 631 (8021), 563–569. <https://doi.org/10.1038/s41586-024-07602-x>.
- Parida, B.R., Pandey, A.C., Patel, N.R., 2020. Greening and browning trends of vegetation in India and their responses to climatic and non-climatic drivers. *Climate* 8 (8), 92. <https://doi.org/10.3390/cli8080092>.
- Pasha, S.V., Dadhwal, V.K., 2024. National analysis on variations in estimates of forest cover dynamics over India (2001–2020) using multiple techniques and data sources. *Spat. Inf. Res.* 32 (4), 451–461. <https://doi.org/10.1007/s41324-024-00570-4>.
- Peñuelas, J., Ciais, P., Canadell, J.G., Janssens, I.A., Fernández-Martínez, M., Carnicer, J., Sardans, J., et al., 2017. Shifting from a fertilization-dominated to a warming-dominated period. *Nat. Ecol. Evol.* 1 (10), 1438–1445. <https://doi.org/10.1038/s41559-017-0274-8>.
- Qin, Y., Xiao, X., Wigneron, J.P., Ciais, P., Brandt, M., Fan, L., Moore III, B., et al., 2021. Carbon loss from forest degradation exceeds that from deforestation in the Brazilian Amazon. *Nat. Clim. Chang.* 11 (5), 442–448. <https://doi.org/10.1038/s41558-021-01026-5>.
- Rascher, U., Alonso, L., Burkart, A., Cilia, C., Cogliati, S., Colombo, R., Zemek, F., et al., 2015. Sun-induced fluorescence: a new probe of photosynthesis: first maps from the imaging spectrometer HyPlant. *Glob. Chang. Biol.* 21 (12), 4673–4684. <https://doi.org/10.1111/gcb.13017>.
- Reddy, C.S., Saranya, K.R.L., Pasha, S.V., Satish, K.V., Jha, C.S., Diwakar, P.G., Murthy, Y.K., et al., 2018. Assessment and monitoring of deforestation and forest fragmentation in South Asia since the 1930s. *Glob. Planet Change* 161, 132–148. <https://doi.org/10.1016/j.gloplacha.2017.10.007>.
- Reichstein, M., Bahn, M., Ciais, P., Frank, D., Mahecha, M.D., Seneviratne, S.I., Wattenbach, M., et al., 2013. Climate extremes and the carbon cycle. *Nature* 500 (7462), 287–295. <https://doi.org/10.1038/nature12350>.
- Ruehr, S., Keenan, T.F., Williams, C., Zhou, Y., Lu, X., Bastos, A., Terrer, C., et al., 2023. Evidence and attribution of the enhanced land carbon sink. *Nat. Rev. Earth Environ.* 4 (8), 518–534. <https://doi.org/10.1038/s43017-023-00456-3>.
- Sannigrahi, S., Pilla, F., Basu, B., Basu, A.S., Sarkar, K., Chakraborti, S., Roy, P.S., et al., 2020. Examining the effects of forest fire on terrestrial carbon emission and ecosystem production in India using remote sensing approaches. *Sci. Total Environ.* 725, 138331. <https://doi.org/10.1016/j.scitotenv.2020.138331>.
- Santoro, M., Cartus, O., Carvalhais, N., Rozendaal, D.M., Avitabile, V., Araza, A., Willcock, S., et al., 2021. The global forest above-ground biomass pool for 2010 estimated from high-resolution satellite observations. *Earth Syst. Sci. Data* 13 (8), 3927–3950. <https://doi.org/10.5194/essd-13-3927-2021>.
- Sarmah, S., Singha, M., Wang, J., Dong, J., Burman, P.K.D., Goswami, S., Niu, S., et al., 2021. Mismatches between vegetation greening and primary productivity trends in South Asia—a satellite evidence. *Int. J. Appl. Earth Observ. Geoinf.* 104, 102561. <https://doi.org/10.1016/j.jag.2021.102561>.
- Seneviratne, S.I., Zhang, X., Adnan, M., Badi, W., Dereczynski, C., Di Luca, A., Zhou, B., et al. (2021). Weather and climate extreme events in a changing climate (Chapter 11). [10.1017/9781009157896.013](https://doi.org/10.1017/9781009157896.013).
- Sharma, A., Goyal, M.K., 2018. Assessment of ecosystem resilience to hydroclimatic disturbances in India. *Glob. Chang. Biol.* 24 (2), e432–e441. <https://doi.org/10.1111/gcb.13874>.
- Shekhar, A., Buchmann, N., Gharun, M., 2022. How well do recently reconstructed solar-induced fluorescence datasets model gross primary productivity? *Remote Sens. Environ.* 283, 113282. <https://doi.org/10.1016/j.rse.2022.113282>.
- Shi, H., Tian, H., Pan, N., Reyer, C.P., Ciais, P., Chang, J., Yang, J., et al., 2021. Saturation of global terrestrial carbon sink under a high warming scenario. *Glob. Biogeochem. Cycles* 35 (10), e2020GB006800. <https://doi.org/10.1029/2020GB006800>.
- Singh, A., Abhishek, K., Kuttippurath, J., Raj, S., Mallick, N., Chander, G., Dixit, S., 2022. Decadal variations in CO₂ during agricultural seasons in India and role of management as sustainable approach. *Environ. Technol. Innov.* 27, 102498. <https://doi.org/10.1016/j.eti.2022.102498>.
- Smith, B., Wärlind, D., Arneth, A., Hickler, T., Leadley, P., Siltberg, J., Zaehle, S., 2014. Implications of incorporating N cycling and N limitations on primary production in an individual-based dynamic vegetation model. *Biogeosciences* 11 (7), 2027–2054. <https://doi.org/10.5194/bg-11-2027-2014>.
- Song, J., Zhou, S., Yu, B., Li, Y., Liu, Y., Yao, Y., Fu, B., et al., 2024. Serious underestimation of reduced carbon uptake due to vegetation compound droughts. *NPJ Clim. Atmos. Sci.* 7 (1), 23. <https://doi.org/10.1038/s41612-024-00571-y>.
- Sparsha, S., Parida, B.R., 2024. Vegetation browning trend progressively leading to forest degradation in eastern Himalaya in response to climatic and anthropogenic drivers. *Remote Sens. Appl. Soc. Environ.* 35, 101209. <https://doi.org/10.1016/j.rsase.2024.101209>.
- Tao, S., Chave, J., Frison, P.L., Le Toan, T., Ciais, P., Fang, J., Saatchi, S., et al., 2022. Increasing and widespread vulnerability of intact tropical rainforests to repeated droughts. *Proc. Natl. Acad. Sci.* 119 (37), e2116626119. <https://doi.org/10.1073/pnas.2116626119>.
- Walther, S., Voigt, M., Thum, T., Gonsamo, A., Zhang, Y., Köhler, P., Guanter, L., et al., 2016. Satellite chlorophyll fluorescence measurements reveal large-scale decoupling of photosynthesis and greenness dynamics in boreal evergreen forests. *Glob. Chang. Biol.* 22 (9), 2979–2996. <https://doi.org/10.1111/gcb.13200>.
- Wang, S., Zhang, Y., Ju, W., Chen, J.M., Ciais, P., Pescatti, A., Peñuelas, J., et al., 2020. Recent global decline of CO₂ fertilization effects on vegetation photosynthesis. *Science* (1979) 370 (6522), 1295–1300. <https://doi.org/10.1126/science.abb7772>.
- Wang, B., Xue, S., Niu, Z., 2023. Increasing trend in ecosystem-scale photosynthetic efficiency in the Yellow River Basin since 2000 caused by afforestation and climate change. *Ecoscience* 30 (3–4), 223–233. <https://doi.org/10.1080/11956860.2024.2303187>.
- Wei, F., Wang, S., Fu, B., Wang, L., Zhang, W., Wang, L., Fensholt, R., et al., 2022. Divergent trends of ecosystem-scale photosynthetic efficiency between arid and humid lands across the globe. *Glob. Ecol. Biogeogr.* 31 (9), 1824–1837. <https://doi.org/10.1111/gcb.13561>.
- Wigneron, J.P., Ciais, P., Li, X., Brandt, M., Canadell, J.G., Tian, F., Fensholt, R., et al., 2024. Global carbon balance of the forest: satellite-based L-VOD results over the last decade. *Front. Remote Sens.* 5, 1338618. <https://doi.org/10.3389/frsen.2024.1338618>.
- Wigneron, J.P., Fan, L., Ciais, P., Bastos, A., Brandt, M., Chave, J., Fensholt, R., et al., 2020. Tropical forests did not recover from the strong 2015–2016 El Niño event. *Sci. Adv.* 6 (6), eaay4603. <https://doi.org/10.1126/sciadv.aay4603>.
- Winkler, A.J., Myneni, R.B., Hannart, A., Sitch, S., Haverd, V., Lombardo, D., Brovkin, V., et al., 2021. Slowdown of the greening trend in natural vegetation with further rise in atmospheric CO₂. *Biogeosciences* 18 (17), 4985–5010. <https://doi.org/10.5194/bg-18-4985-2021>.
- Wu, J., Wang, D., Li, L.Z., Zeng, Z., 2022. Hydrological feedback from projected Earth greening in the 21st century. *Sustain. Horiz.* 1, 100007. <https://doi.org/10.1016/j.horiz.2022.100007>.
- Yan, D., Scott, R.L., Moore, D.J.P., Biederman, J.A., Smith, W.K., 2019. Understanding the relationship between vegetation greenness and productivity across dryland ecosystems through the integration of PhenoCam, satellite, and eddy covariance data. *Remote Sens. Environ.* 223, 50–62. <https://doi.org/10.1016/j.rse.2018.12.029>.
- Yan, Y., Liu, Z., Chen, L., Chen, X., Lin, K., Zeng, Z., Ma, Z., et al., 2025. Earth greening and climate change reshaping the patterns of terrestrial water sinks and sources. *Proc. Natl. Acad. Sci.* 122 (11), e2410881122. <https://doi.org/10.1073/pnas.2410881122>.
- Yang, H., Ciais, P., Frappart, F., Li, X., Brandt, M., Fensholt, R., Wigneron, J.P., et al., 2023. Global increase in biomass carbon stock dominated by growth of northern young forests over past decade. *Nat. Geosci.* 16 (10), 886–892. <https://doi.org/10.1038/s41561-023-01274-4>.
- Zeng, Y., Hao, D., Park, T., Zhu, P., Huete, A., Myneni, R., Chen, M., et al., 2023. Structural complexity biases vegetation greenness measures. *Nat. Ecol. Evol.* 7 (11), 1790–1798. <https://doi.org/10.1038/s41559-023-02187-6>.
- Zhang, Y., Liu, X., Wang, L., Zeng, X., Zhao, L., Wu, X., et al., 2024. Reductions in forest resilience: unraveling the decoupling between gross primary productivity and photosynthetic efficiency. *Geophys. Res. Lett.* 51 (16), e2024GL110148. <https://doi.org/10.1029/2024GL110148>.
- Zhao, Q., Zhu, Z., Zeng, H., Zhao, W., Myneni, R.B., 2020. Future greening of the Earth may not be as large as previously predicted. *Agric. For. Meteorol.* 292, 108111. <https://doi.org/10.1016/j.agrformet.2020.108111>.
- Zhao, Z., Ciais, P., Wigneron, J.P., Santoro, M., Brandt, M., Kleinschroth, F., Li, W., et al., 2024. Central African biomass carbon losses and gains during 2010–2019. *One Earth* 7 (3), 506–519. <https://doi.org/10.1016/j.oneear.2024.01.02101>.